PERGAMON

Planetary and Space Science 47 (1999) 85–106

Planetary and Space Science

Three years of Galileo dust data: II. 1993–1995

H. Krüger[a,*], E. Grün[a], D.P. Hamilton[b], M. Baguhl[a], S. Dermott[c], H. Fechtig[a], B.A. Gustafson[c], M.S. Hanner[d], M. Horányi[e], J. Kissel[a], B.A. Lindblad[f], D. Linkert[a], G. Linkert[a], I. Mann[g], J.A.M. McDonnell[h], G.E. Morfill[i], C. Polanskey[d], R. Riemann[j], G. Schwehm[j], R. Srama[a], H.A. Zook[k]

[a] *Max-Planck-Institut für Kernphysik, 69029 Heidelberg, Germany*
[b] *University of Maryland, College Park, MD 20742-2421, U.S.A.*
[c] *University of Florida, Gainesville, FL 32611, U.S.A.*
[d] *Jet Propulsion Laboratory, Pasadena, California 91109, U.S.A.*
[e] *Laboratory for Atmospheric and Space Physics, Univ. Of Colorado, Boulder, CO 80309, U.S.A.*
[f] *Lund Observatory, 221 Lund, Sweden*
[g] *Max-Planck-Institute für Aeronomie, 37191 Katlenburg-Lindau, Germany*
[h] *University of Kent, Canterbury CT2 7NR, U.K.*
[i] *Max-Planck-Institut für Extraterrestrische Physik, 85748 Garching, Germany*
[j] *ESTEC, 2200 AG Noordwijk, The Netherlands*
[k] *NASA Johnson Space Center, Houston, Texas 77058, U.S.A.*

Received 9 April 1998; received in revised form 15 April 1998; accepted 6 September 1998

Abstract

Between January 1993–December 1995, the Galileo spacecraft traversed interplanetary space between Earth and Jupiter and arrived at Jupiter on 7 December 1995. The dust instrument onboard the spacecraft was operating during most of the time and data from the instrument were obtained via memory readouts which occurred at rates between twice per day and once per week. All events were classified by an onboard program into 24 categories. Noise events were usually restricted to the lowest categories (class 0). During Galileo's passage through Jupiter's radiation belts on 7 December 1995, several of the higher categories (classes 1 and 2) also show evidence for contamination by noise. The highest categories (class 3) were noise-free all the time. A relatively constant impact rate of interplanetary and interstellar (big) particles of 0.4 impacts per day was detected over the whole three-year time span. In the outer solar system (outside about 2.6 AU) they are mostly of interstellar origin, whereas in the inner solar system they are mostly interplanetary particles. Within about 1.7 AU from Jupiter intense streams of small dust particles were detected with impact rates of up to 20,000 per day whose impact directions are compatible with a Jovian origin. Two different populations of dust particles were detected in Jovian magnetosphere: small stream particles during Galileo's approach to the planet and big particles concentrated closer to Jupiter between the Galilean satellites. There is strong evidence that the dust stream particles are orders of magnitude smaller in mass and faster than the instrument's calibration, whereas the calibration is valid for the big particles. Because the data transmission rate was very low, the complete data set for only a small fraction (2525) of all detected particles could be transmitted to Earth; the other particles were only counted. Together with the 358 particles published earlier, information about 2883 particles detected by the dust instrument during Galileo's six years' journey to Jupiter is now available.

1. Introduction

The dust sensors onboard the Galileo and Ulysses spacecraft are highly sensitive impact ionization detectors. The two nearly identical sensors have been described in detail by Grün et al. (1992a,b; 1995a). Results from the dust experiments on both spacecraft have been published frequently: Grün et al. (1992c) published early results from both missions, and dust originating from comets and asteroids has been considered by Riemann and Grün (1992), Hamilton and Burns (1992) and Grün et al. (1994). Dust streams originating from the Jovian system and interstellar dust particles have been discovered with the Ulysses detector (Grün et al., 1993). these were later confirmed by Galileo (Baguhl et al., 1995; Grün et al., 1996a). Grün et al. (1996b) discuss dust particles detected a few days around Galileo's Io flyby on 7 December 1995.

* Corresponding author. Fax: +49 6221 516 324; e-mail: krueger@galileo.mpi-hd.mpg.de

0032–0633/99/$ - see front matter
PII: S0032–0633(98)00097–X

During its orbital tour within the Jovian magnetosphere Galileo has demonstrated the electromagnetic interaction of submicron-sized dust particles with Jupiter's magnetic field (Grün et al., 1997; 1998). The data from both instruments—Galileo and Ulysses—have been used to model the interplanetary meteoroid populations (Divine, 1993; Grün et al., 1997c) and to compare the mass distribution of interstellar particles derived from in-situ measurements with that obtained from astronomical observations (Baguhl et al., 1996; Landgraf and Grün, 1998). Finally, Zook et al. (1996) and Horányi et al. (1997) used data from both spacecraft to model the Jovian dust streams.

This is the fourth paper in a series dedicated to presenting both raw and reduced data from Galileo and Ulysses dust instruments. Grün et al. (1995a; hereafter, Paper I) described the reduction process of Galileo and Ulysses data. Papers II and III (Grün et al., 1995b,c) contain the data sets from the initial three and two years of the Galileo and Ulysses missions, respectively. In the case of Galileo the time period covered (Paper II) was December 1989–December 1992. In the current paper we extend the Galileo data set from January 1993–December 1995. In a companion paper (Krüger et al., 1998, Paper V) we publish the Ulysses data set for the same time period. The main data products are a table of the impact rate of all impacts determined from the particle accumulators and a table of both raw and reduced data of all 'big' impacts received on the ground. The information presented in these papers is similar to data which we are submitting to the various data archiving centers (Planetary Data System, NSSDC, etc.). The only difference is that the paper version does not contain the full data set of the large numbers of 'small' particles. Electronic access to the full data set is also possible via the world wide web: http://galileo.mpi-hd.mpg.de.

This paper is organised similarly to Paper II. Section 2 gives a brief overview of the Galileo mission until the end of 1995, the dust instrument and lists important mission events during the 1993–95 period. A description of the Galileo dust data set for 1993–95, together with a discussion of the detected impact rate, is given in Sect. 3. Section 4 analyses and discusses various characteristics of the new data set. We dedicate Section 5 to an analysis of the dust particles and the noise events detected around Io flyby on 7 December 1995. Finally, Section 6 summarizes our results.

2. Mission and instrument operation

Galileo was launched on 18 October 1989. During the initial three years of the mission, Galileo was in the inner solar system and had flybys of Venus, Earth and the asteroid Gaspra. After its second Earth flyby in December 1992, Galileo had enough energy to leave the inner solar system, fly by the asteroid Ida, and reach

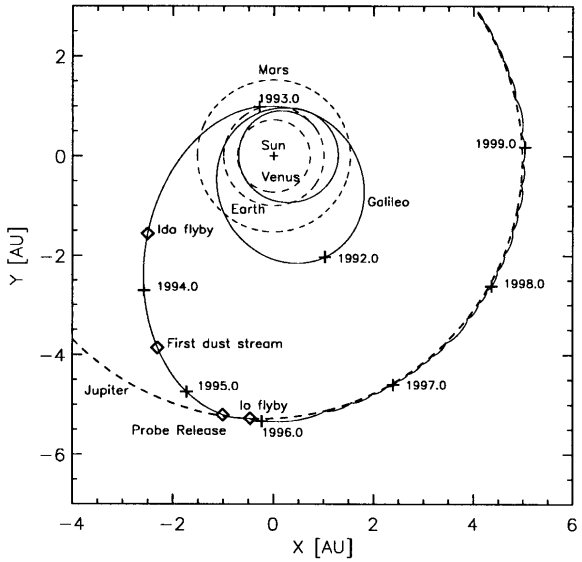

Fig. 1. Galileo's interplanetary trajectory from launch until the end of 1999 (solid line) and the orbits of Venus, Earth, Mars and Jupiter (dashed lines). Crosses mark the spacecraft position at the beginning of each year, diamonds indicate special events in the time interval 1993–95 which is the subject of this paper.

Jupiter in December 1995. Galileo's interplanetary trajectory is shown in Fig. 1 with a few important events indicated: on 28 August 1993, Galileo flew by the asteroid Ida; the atmospheric entry probe was released from the Galileo orbiter on 13 July 1995; on 7 December 1995 Galileo arrived at Jupiter and—after a swing by at Io—was injected into a highly elliptical orbit about the planet. Orbital elements of the Galileo trajectory are provided in Table 1. Galileo now performs regular close flybys of Jupiter's Galilean satellites. A detailed description of the Galileo mission and the spacecraft are given by Johnson et al. (1992) and D'Amario et al. (1992).

Galileo is a dual spinning spacecraft with an antenna that points antiparallel to the positive spin axis. During most of the initial three years of the mission the antenna pointed towards the Sun (cf. Fig. 2 in Paper II). Since

Table 1
Heliocentric orbital elements of Galileo's interplanetary trajectory for 1993–95. The positional error is less than 500,000 km (=0.003 AU) from 1 Jan 1993–1 Jan. 1995. The error increases to 2,500,000 km (=0.02 AU) by mid 1995 and to 10,000,000 km (=0.07 AU) by end of 1995. The increasing error is due to the strong influence of Jupiter

Epoch	4 Sept. 1993, 16:48:00
Perihelion	0.98849 AU
Eccentricity	0.68548
Inclination	1.5169°
Long. of asc. node	255.99°
Arg. of perihelion	186.71°
Mean anomaly	46.953°
True anomaly	130.40°

1993, the antenna usually points towards Earth. Deviations from the Earth pointing direction between January 1993–December 1995 are shown in Fig. 2.

The Dust Detector System (DDS) is mounted on the spinning section of Galileo and the sensor axis is offset by an angle of 60° from the positive spin axis (Fig. 3; an angle of 55° has been erroneously used earlier). The rotation angle measures the viewing direction of the dust

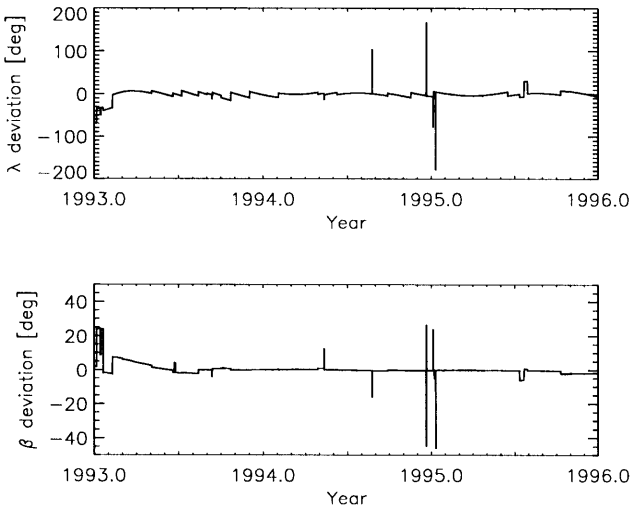

Fig. 2. Spacecraft attitude: deviation of the antenna pointing direction (i.e., negative spin axis) from the Earth direction. The angles are given in ecliptic longitude (top) and latitude (bottom, equinox 1950.0).

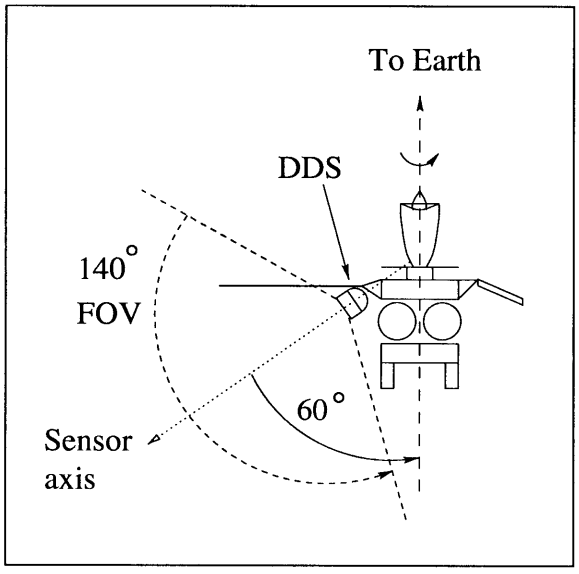

Fig. 3. Orientation of Galileo and DDS: the antenna (top) points towards Earth and the dust detector (DDS) largely faces the anti-Earth hemisphere. The sensor axis has an angle of 60° from the positive spin axis (i.e., the anti-Earth direction). During one spin revolution of the spacecraft, the sensor axis scans a cone with 120° opening angle. The dust detector itself has 140° field of view (FOV). The sensor orientation shown corresponds to a rotation angle of 270° if viewed from the north ecliptic pole.

sensor at the time of a dust particle impact. During one spin revolution of the spacecraft the rotation angle scans through a complete circle of 360°. At rotation angles of 90° and 270°, the sensor axis lies nearly in the ecliptic plane, and at 0° it is close to ecliptic north. DDS rotation angles are taken positive around the negative spin axis of the spacecraft. This is done to easily compare Galileo impact spin angle data with those taken by Ulysses, which, unlike Galileo, has its positive spin axis pointed towards Earth. DDS has a 140° wide field of view and during one spin revolution of the spacecraft the sensor axis scans a cone with 120° opening angle towards the anti-Earth direction. Dust particles that arrive from within 10° of the positive spin axis (anti-Earth direction) can be sensed at all rotation angles, whereas those that arrive at angles from 10–130° from the positive spin axis can only be detected over a limited range of rotation angles.

During most of the interplanetary cruise (i.e., prior to 7 December 1995), we received DDS data as instrument memory-readouts (MROs). The MROs returned event data which had accumulated over time in the instrument memory. Initially, an MRO contained 14 instrument data frames (with each frame comprising the complete data set of an impact or noise event, consisting of 128 bits, plus ancillary and engineering data). Since June 1990, when DDS was reprogrammed for the first time after launch, an MRO contains 46 instrument data frames (cf. Paper I). DDS time-tags each impact event with an 8 bit word allowing for the identification of 256 unique times. The step size of this time word was also changed from 1.1 to 4.3. h in the June 1990 reprogramming to allow for longer time periods between MROs without loss of the impact time information. The total accumulation time is now 256×4.3 h $= 46$ days, after which the time word is reset and the time labels of older impact events become ambiguous. MROs usually occurred twice a week which was sufficient to get the time information of the impact events transmitted to Earth within the 46 day period. The accuracy, however, with which the impact time can be determined, is limited to 4.3 h.

For two periods of a few hours around Io flyby on 7 December 1995, the instrument was read-out every few minutes, the data were stored on Galileo's tape recorder and transmitted to Earth during the following months (record mode). Seven different instrument data frames were read-out this way within about one min (with six frames containing the information of the six most recent impact events, the so-called A range; cf. Paper I). although fewer data frames were read-out in this manner at a time, the number of new events that could be transmitted to Earth in a given time period was much larger than with MROs due to the higher read-out cycle. Furthermore, in record mode the read-out cycle determines the accuracy of the impact time to within a few minutes, much better than with MROs.

Table 2 lists significant mission and dust instrument events for the period 1993–95. A comprehensive list of earlier events can be found in Paper II. After Galileo's second Earth flyby on 8 December 1992, DDS was brought into its nominal operational mode for the rest of the interplanetary cruise to Jupiter: the channeltron voltage was set to 1020 V (HV = 2), the event definition status was set such that the channeltron or the ion-collector channel can independently initiate a measurement cycle (EVD = C, I) and the detection thresholds for ion-collector, channeltron, electron-channel and entrance grid were set (SSEN = 0, 0, 1, 1). Detailed descriptions of these symbols are given in Paper I.

The operational mode of DDS was changed several times during noise tests between 1993–1995: starting from the nominal configuration described above, all tests have been achieved with the same instrument settings. The following changes of the instrument configuration were

Table 2
Galileo mission and dust detector (DDS) configuration, tests and other events. See text for details. Only selected events are given before 1993

Year-day	Date	Time	Event
89-291	18 Oct. 1989	16:52	Galileo launch
92-343	08 Dec. 1992	15:09	Galileo second Earth flyby
92-343	08 Dec. 1992	16:09	DDS configuration: HV = 2, EVD = C, I, SSEN = 0, 0, 1, 1
92-357	22 Dec. 1992	14:59	DDS first MRO after second Earth flyby
93-166	15 Jun. 1993		Galileo 80 bytes MRO Format
93-240	28 Aug. 1993	16:52	Galileo Ida flyby
93-288	15 Oct. 1993	05:42	DDS noise test start
93-301	28 Oct. 1993	03:27	DDS noise test end
93-320	16 Nov. 1993	03:16	DDS noise test start
93-328	24 Nov. 1993	01:58	DDS noise test end
93-355	21 Dec. 1993	21:07	DDS noise test start
94-006	06 Jan. 1994	20:27	DDS noise test end
94-195	14 Jul. 1994	11:00	DDS last MRO before reprogramming
94-195	14 Jul. 1994	14:35	DDS counters reset, new event classification program
94-196	15 Jul. 1994	02:00	DDS first MRO after reprogramming
94-197	16 Jul. 1994		Galileo start SL 9 observations, duration: 6 days
94-210	29 Jul. 1994	00:14	DDS noise test start
94-219	07 Aug. 1994	08:14	DDS noise test end
94-300	27 Oct. 1994	02:38	DDS noise test start
94-312	08 Nov. 1994	03:08	DDS noise test end
95-019	19 Jan. 1995	22:56	DDS noise test start
95-029	29 Jan. 1995	03:09	DDS noise test end
95-035	04 Feb. 1995	17:44	Galileo phase 1 software load
95-110	20 Apr. 1995	15:19	DDS noise test start
95-119	29 Apr. 1995	16:31	DDS noise test end
95-184	03 Jul. 1995	04:30	DDS last MRO before probe release
95-194	13 Jul. 1995		Galileo probe release
95-205	25 Jul. 1995	06:54	DDS configuration for ODM wake-up burn: HV = 0
95-205	25 Jul. 1995	13:00	DDS configuration: HV = 2
95-208	27 Jul. 1995	06:54	DDS configuration for ODM wake-up burn: HV = 0
95-208	27 Jul. 1995	13:00	DDS configuration: HV = 2
95-209	28 Jul. 1995	06:00	DDS first MRO after probe release
95-221	09 Aug. 1995	06:14	DDS noise test start
95-231	19 Aug. 1995	05:40	DDS noise test end
95-340	06 Dec. 1995	05:00	DDS last MRO before Io and Jupiter flybys
95-340	06 Dec. 1995	05:40	DDS configuration: HV = 1, EVD = I, SEN = 2, 0, 2, 2
95-341	07 Dec. 1995	15:21	Galileo start record data (21 bps DDS data)
95-341	07 Dec. 1995	17:46	Galileo Io flyby, altitude: 892 km
95-341	07 Dec. 1995	18:25	Galileo end record data
95-341	07 Dec. 1995	21:54	Galileo Jupiter closest approach, altitude: 215,000 km
95-341	07 Dec. 1995	23:22	Galileo start record data (21 bps DDS data)
95-341	07 Dec. 1995	23:25	DDS configuration: HV = off
95-342	08 Dec. 1995	00:27	Galileo start orbit insertion burn, duration: 49 min
95-342	08 Dec. 1995	01:26	Galileo end record data
95-362	28 Dec. 1995	11:00	DDS MRO covering Io and Jupiter flybys

Abbreviations used: MRO: DDS memory read-out; HV: channeltron high voltage step; EVD: event definition, ion- (I), channeltron- (C), or electron-channel (E); SSEN: detection thresholds, ICP, CCP, ECP and PCP; ODM: orbit deflection maneuver; SL 9: comet Shoemaker-Levy 9.

applied at 2–3-day intervals: (a) increase the channeltron high voltage by one digital step (HV = 3); (b) reset the channeltron high voltage to its nominal value (HV = 2); (c) set the event definition status such that the channeltron, the ion collector and the electron-channel can each, independently, initiate a measurement cycle (EVD = C, I, E); (d) set the thresholds for all channels to their lowest levels (SSEN = 0, 0, 0, 0); (e) reset the thresholds and the event definition status to their nominal configuration (SSEN = 0, 0, 1, 1, EVD = C, I). Note that after step (e), DDS is brought back to its nominal configuration. No detectable changes in the noise characteristics were revealed by these noise tests.

The instrument memory was not read out between 3–28 July 1995 and no DDS data could be obtained. In this period the atmospheric entry probe was released from the orbiter and a propulsion system burn occurred during the orbit deflection maneuver (ODM) of the orbiter. Within the Jovian magnetosphere a strong increase in the high energy electron flux was expected close to Jupiter. To save the instrument from the hazards associated with Jupiter's radiation environment, the channeltron voltage was reduced and the detection thresholds were increased on 6 December 1995, 5:40 h (HV = 1, EVD = I, SSEN = 2, 0, 2, 2) at a distance of 30 R_J from Jupiter (Jupiter radius, R_J = 71,492 km). On 7 December 1995, 23:25 h, shortly before insertion of Galileo into Jupiter orbit, the channeltron high voltage was switched off. The Io and Jupiter flybys will be discussed in detail in Section 5.

3. Impact events and classification scheme

DDS classifies all events—real impacts of dust particles and noise events—into one of 24 different categories (six amplitude ranges for the charge measured on the ion collector grid and four event classes) and counts them in 24 corresponding accumulators (Paper I). Most of the 24 categories are relatively free from noise and only sensitive to real dust impacts, except for extreme situations like the crossings of the radiation belts of Earth, Venus (Paper II) and Jupiter (7 December 1995, Sect. 5). During most of Galileo's initial three years of interplanetary cruise since launch, only the lowest amplitude and class categories—AC01 (event class 0, amplitude range 1, AR1), AC11, and AC02—were contaminated by noise events (Paper II).

In a detailed analysis of the Ulysses data set published in Paper III, Baguhl et al. (1993) identified a large number of 'small' impacts in the three lowest categories. They deduced a modified event classification scheme that allows for a better discrimination between noise events and real dust impacts. The modified scheme was loaded to the instrument computer on board Galileo during the second reprogramming of DDS on 14 July 1994 and is shown in Table 3. The definition of class 3 remains unchanged with respect to the old scheme published in Paper I. Classes 1 and 2 are now divided into two subclasses. With the modified scheme, noise events are now usually restricted to class 0. Class 3 always contains good dust impacts (two AC31 events were rejected which occurred during a noise test on 15 August 1995 because they did not fulfill the class 3 classification criteria). After the 14 July 1994 reprogramming, all class 1 and 2 events detected in the low radiation environment of interplanetary space are true dust impacts. Dust impacts which do not fulfill the criteria of classes 1, 2 or 3 are automatically assigned class 0. Therefore, class 0 may still contain good dust impacts, especially in the higher amplitude ranges. Although noise events are now normally restricted to class 0, classes 1 and 2 are also contaminated by noise in extreme radiation environments (Section 5). With the modified scheme, the mass sensitivity of the instrument could be improved by a factor of eight and the number of dust particles identified in the Ulysses data set from October 1990–December 1992 was enhanced from 333 to 968 (Baguhl et al., 1993).

Table 4 lists the number of all dust impacts identified with the Galileo dust sensor between 1 January 1993–31 December 1995. Before 14 July 1994, the particles were classified with the old classification scheme whereas afterwards the modified scheme was applied. The number of impacts is typically given in intervals of about one week, depending on the occurrence of MROs. When the frequency of MROs was higher or when no impact was recorded, MROs were put together. Typically, MROs occurred twice per week. In interplanetary space where the impact rate was roughly one impact per two days (see below) this was sufficient to receive the complete information of all particles. During the occurrence of dust streams when the impact rates in the lowest amplitude range (AR1) were higher by several orders of magnitude the full information of only a small fraction of all detected particles could be transmitted to Earth. In this case the impact rates had to be deduced from the accumulators.

The frequency of MROs limits the maximum impact rate of dust particles that can be determined from the accumulators. If an unknown number of accumulator overflows occurs between individual MROs the number of particles and, hence, the impact rate deduced is only a lower limit to the real dust impact rate. With MROs occurring every few days, impact rates of up to 100 per day could be determined from the accumulators. Between the end of July and October 1995, when the strongest dust streams were observed, MROs were transmitted to Earth usually daily, sometimes even more frequently. During the occurrence of the most intensive dust streams MROs were split-up and transmitted in two segments separated by about 25 min. This way rates of up to 20,000 impacts per day could be determined from the

Table 3
Galileo DDS on board classification scheme as derived from the analysis of Baguhl et al. (1993). This scheme was implemented in the instrument computer onboard Galileo during the 14 July 1994 reprogramming. Note that classes 1 and 2 are now divided into two different subclasses which are mutually exclusive. See Paper I for a detailed explanation of the instrument parameters

Parameters	CLN = 0	CLN = 1	CLN = 2	CLN = 3
Iongrid amplitude (IA)	IA > 0	IA > 0	IA > 0	IA > 0
Target amplitude (EA)	or EA > 0	EA > 0	EA > 0	EA > 0
Channeltron amplitude (CA)	or CA > 0	CA > 0	CA > 0	CA > 0
Flighttime target-iongrid (EIT)		EIT = 0 or EIT = 15	3 < EIT < 15	3 < EIT < 15
Target-iongrid coincidence (EIC)		EIC = 1	EIC = 0	EIC = 0
Channeltron-iongrid coincidence (ICC)			ICC = 1	ICC = 1
Noise counter of:				
target (EN)			EN ⩽ 8	EN ⩽ 8
iongrid (IN)			IN ⩽ 14	IN ⩽ 2
channeltron (CN)			CN ⩽ 14	CN ⩽ 2
EA risetime (ET)				1 ⩽ ET ⩽ 15
IA risetime (IT)				1 ⩽ IT ⩽ 15

accumulators over such short time intervals. Entries in Table 4 indicated by '#' signs, give the number of impacts determined from the accumulators in the lowest amplitude range over the 25 min interval. No overflows of the accumulators for the higher amplitude ranges (AR2 to AR6) occurred between MROs even during the most intensive dust streams. During the strongest dust streams, however, the effective measurement time for such particles was significantly reduced due to deadtime (cf. Fig. 9).

In this paper the terms 'small' and 'big' do *not* have the same meaning as in Paper II. Here we call all particles in classes 1, 2 and 3 in the amplitude ranges 2 and higher (AR2 to AR6) 'big'. Particles in the lowest amplitude range (AR1) are called 'small'. This distinction separates the small Jovian dust stream particles from big particles of interplanetary or interstellar origin (cf. Fig. 9).

The total dust impact rate recorded by DDS from 1993–95 is shown in Fig. 4. During this three year time span, the average impact rate of big particles (AR2–AR6) was rather constant, with 0.4 impacts per day. From the beginning of 1993 until the first half of 1994 , the average impact rate of small particles (AR1) was about an order of magnitude lower. Later the small particles dominated the overall impact rate. No increase in the impact rate was detected during the Ida flyby on 28 August 1993 and during the passage through the asteroid belt. This is consistent with the absence of an enhance impact rate during the Gaspra flyby two years earlier, and it is in agreement with the predictions of Hamilton and Burns (1992). DDS detected the first Jovian dust stream on 25 June 1994 with a peak rate of 10 impacts per day. At this time Galileo was still about 1.7 AU away from Jupiter. During the dust streams detected later and closer to Jupiter an impact rate of up to 20,000 per day has been detected. Although such an impact rate is close to the technical limit of Galileo, the data indicate that undetected accumulator overflows did not occur frequently. A detailed discussion of the Jovian dust streams detected with DDS is given by Grün et al. (1996a).

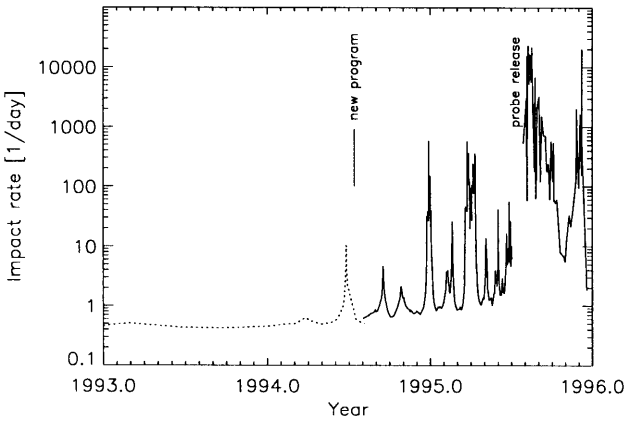

Fig. 4. Total dust impact rate detected by DDS as a function of time before (dotted line) and after the reprogramming on 14 July 1994 (solid line). The dotted line is a running average over 9 impacts. The data gap in summer 1995 is due to the release of Galileo's atmospheric entry probe.

Table 5 lists all 395 big particles detected in classes 1–3 between January 1993–December 1995 for which the complete information exists (Note that this table includes 47 class 1 and 2 events around Io and Jupiter flybys which are possibly noise events; see Section 5). We do not list the small particles (AR1) in Table 5 because their masses and velocities are outside the calibrated range of DDS. The stream particles are believed to be about 10 nm in

size and their velocities exceed 200 km/s (Zook et al., 1996). Any mass and velocity calibration of these particles would be unreliable. The complete information of a total of 2130 small particles has been transmitted to Earth from 1993–95. The full data set of all 2525 small and big particles is available in electronic form.

In Table 5, dust particles are identified by their sequence number and their impact time. Gaps in the sequence number are due to the omission of the small particles. The event category—class (CLN) and amplitude range (AR)—are given. Raw data as transmitted to Earth are displayed in the next columns: sector value (SEC) which is the spacecraft spin orientation at the time of impact, impact charge numbers (IA, EA, CA) and rise times (IT, ET), time difference and coincidence of electron and ion signals (EIT, EIC), coincidence of ion and channeltron signal (IIC), charge reading at the entrance grid (PA) and time (PET) between this signal and the impact. Then the instrument configuration is given: event definition (EVD), charge sensing thresholds (ICP, ECP, CCP, PCP) and channeltron high voltage step (HV). See Paper I for further explanation of the instrument parameters.

The next four columns in Table 5 give information about Galileo's orbit: heliocentric distance (R), ecliptic longitude and latitude (LON, LAT) and distance from Jupiter (D_{Jup}). The next column gives the rotation angle (ROT) as described in Section 2. Whenever this value is unknown, ROT is arbitrarily set to 999. This occurs 21 times (80 times in the full data set that includes the small particles). Then follows the pointing direction of DDS at the time of particle impact in ecliptic longitude and latitude (S_{LON}, S_{LAT}). When ROT is not valid, S_{LON} and S_{LAT} are also useless. Mean impact velocity (V) and velocity error factor (VEF, i.e., multiply or divide stated velocity by VEF to obtain upper or lower limits) as well as mean particle mass (M) and mass error factor (MEF) are given in the last columns. For $VEF > 6$, both velocity and mass values should be discarded. This occurs for five impacts. No intrinsic dust charge values are given (see Svestka et al., 1996 for a detailed analysis).

4. Analysis

The positive charge measured on the ion collector, Q_{I}, is the most important impact parameter determined by DDS because it is rather insensitive to noise. Figure 5 shows the distribution of Q_{I} for the full data set (small and big particles) from 1993–95. Ion impact charges have been detected over the entire range of six orders of magnitude that the instrument can measure. Two impacts (about 0.1% of the total) are close to the saturation limit of $Q_{\mathrm{I}} \sim 10^{-8}$ C and may thus constitute lower limits of the actual impact charges. The impact charge distribution of the big particles ($Q_{\mathrm{I}} > 10^{-13}$ C) follows a power law

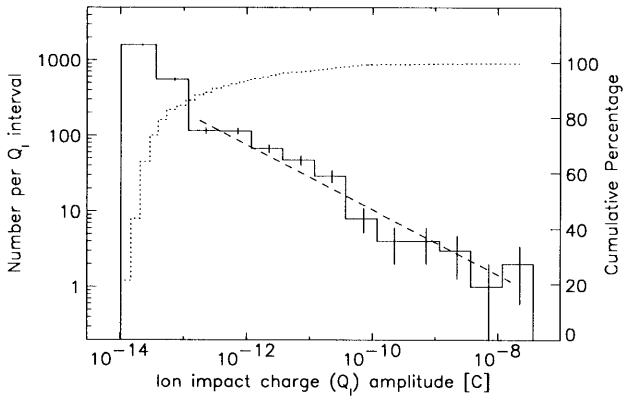

Fig. 5. Amplitude distribution of the impact charge Q_{I} for particles detected between 1993–95. The solid line indicates the number of impacts per charge interval, whereas the dotted line shows the cumulative distribution. Vertical bars indicate the $\sqrt{n}$ statistical fluctuation. A power law fit to the data with $Q_{\mathrm{I}} > 10^{-13}$ C is shown as a dashed line (power law index -0.43).

with index -0.43 and is shown as a dashed line. This slope is steeper than the value of $-1/3$ given for Galileo in Paper II and flatter than the $-1/2$ given for Ulysses in Paper III. It indicates that, on average, Galileo has detected smaller particles in the outer solar system than in the inner solar system. This is in agreement with a larger contribution of interstellar particles further away from the Sun. Note that the Jovian steam particles (AR1) have been excluded from the power law fit.

In Fig. 5, the small particles ($Q_{\mathrm{I}} < 10^{-13}$ C) are put together in two histogram bins. To analyse their behavior in more detail, their number per individual digital step is shown separately in Fig. 6. The distribution flattens for impact charges below 2×10^{-14} C. This indicates that the sensitivity threshold of DDS may not be sharp and the number of impacts with the lowest impact charges Q_{I} may not be complete. The impact charge distribution for these small particles above $Q_{\mathrm{I}} > 2 \times 10^{-14}$ C follows a power law with index -1.9. This indicates that the size distribution of the small stream particles rises steeply towards smaller particles and is much steeper than the distribution of the big particles shown in Fig. 5.

The ratio of the channeltron charge Q_{C} and the ion collector charge Q_{I} is a measure of the channeltron amplification A which is an important parameter for the dust impact identification (Paper I). The in-flight channeltron amplification was determined in Paper II for the initial three years of the Galileo mission. For a channeltron high voltage of 1020 V (HV = 2), the amplification $Q_{\mathrm{C}}/Q_{\mathrm{I}}$ obtained for 10^{-12} C $\leqslant Q_{\mathrm{I}} \leqslant 10^{-10}$C was $A \sim 1.6$. Here we repeat the same analysis for the time period 1993–95 to identify any degrading of the channeltron. Figure 7 shows the charge ratio $Q_{\mathrm{C}}/Q_{\mathrm{I}}$ as a function of Q_{I} for the same high voltage as in Paper II. The charge ratio $Q_{\mathrm{C}}/Q_{\mathrm{I}}$ determined for 10^{-12} C $\leqslant Q_{\mathrm{I}} \leqslant 10^{-10}$ C is $A \sim 1.4$. Thus, no significant aging of the channeltron is detectable. We

Table 4
Overview of dust impacts accumulated with Galileo DDS between 1 January 1993–31 December 1995. Days 94–195 when no data were received due to the instrument reprogramming, is indicated by a horizontal line. The heliocentric distance R, the lengths of the time interval Δt (days) from the previous table entry, and the corresponding numbers of impacts are given for the 24 accumulators. The accumulators are arranged with increasing signal amplitude ranges (AR), with four event classes for each amplitude range (CLN = 0, 1, 2, 3); e.g., AC31 means counter for AR = 1 and CLN = 3. Entries for accumulators that usually contain noise events are marked by '*' signs. Entries marked by '#' denote numbers of impacts counted over 25 min intervals. The Δt in the first line (93-022) is the time interval counted from the last entry in Table 3 in Paper II. The totals of counted impacts, of impacts with complete data, and of all events (noise plus impact events) for the entire period are also given. Note that the totals of counted impacts in amplitude range 1 are not complete due to accumulator overflow during the dust streams

Date	Time	R (AU)	Δt (d)	AC 01	AC 11	AC 21	AC 31	AC 02	AC 12	AC 22	AC 32	AC 03	AC 13	AC 23	AC 33	AC 04	AC 14	AC 24	AC 34	AC 05	AC 15	AC 25	AC 35	AC 06	AC 16	AC 26	AC 36
93-022	16:48	1.136	25.0	*	*	—	2	*	6	1	2	—	3	1	4	—	2	—	1	—	2	1	2	—	1	—	—
93-039	22:53	1.267	17.3	*	*	—	—	*	3	—	1	—	—	—	1	—	—	—	1	—	—	—	—	—	—	—	—
93-061	02:38	1.450	21.2	*	*	—	4	*	3	—	3	—	1	—	3	—	3	—	1	—	—	—	2	—	1	—	—
93-084	03:09	1.660	23.0	*	*	—	2	*	2	—	4	—	—	—	1	—	2	—	1	—	—	—	1	—	—	—	—
93-102	18:24	1.830	18.6	*	*	—	2	*	—	—	1	—	—	—	1	—	—	—	—	—	—	—	—	—	1	—	—
93-116	17:53	1.956	14.0	*	*	—	—	*	2	—	1	—	2	—	3	—	1	—	1	—	—	—	—	—	—	—	1
93-130	16:59	2.080	14.0	*	*	—	—	*	1	—	3	—	—	—	2	—	—	—	—	—	—	—	—	—	—	—	—
93-144	17:03	2.201	14.0	*	*	—	2	*	1	—	1	—	1	—	2	—	—	—	1	—	—	—	—	—	—	—	—
93-152	17:43	2.269	8.0	*	*	—	—	*	1	—	—	—	—	—	1	—	—	—	—	—	—	—	—	—	—	—	—
93-163	19:06	2.362	11.1	*	*	—	—	*	—	—	1	—	—	—	2	—	—	—	—	—	—	—	—	—	—	—	—
93-209	17:41	2.725	45.9	*	*	—	—	*	4	—	2	—	2	—	4	—	—	—	3	—	—	—	—	—	—	—	—
93-222	22:13	2.823	13.2	*	*	—	—	*	—	—	1	—	—	—	1	—	—	—	1	—	—	—	—	—	—	—	—
93-233	11:10	2.899	10.5	*	*	—	—	*	2	—	—	—	—	—	1	—	—	—	2	—	—	—	—	—	—	—	—
93-242	07:27	2.962	8.8	*	*	—	—	*	—	—	1	—	1	—	1	—	—	—	—	—	—	—	—	—	—	—	—
93-259	01:46	3.078	16.8	*	*	—	—	*	—	—	4	—	—	—	3	—	—	—	1	—	—	—	—	—	—	—	—
93-268	06:48	3.140	9.2	*	*	—	—	*	—	—	1	—	—	—	—	—	—	—	—	—	—	—	—	—	—	—	—
93-275	11:51	3.187	7.2	*	*	—	—	*	—	—	1	—	—	—	3	—	—	—	1	—	—	—	—	—	—	—	—
93-284	20:51	3.248	9.4	*	*	—	—	*	1	—	—	—	—	—	1	—	—	—	—	—	—	—	—	—	—	—	—
93-297	23:11	3.331	13.1	*	*	—	1	*	1	—	—	—	—	—	—	—	—	—	1	—	—	—	—	—	—	—	—
93-316	03:20	3.443	18.2	*	*	—	1	*	1	—	1	—	1	—	4	—	—	—	2	—	—	—	—	—	—	—	—
93-324	01:46	3.490	7.9	*	*	—	—	*	1	—	—	—	—	—	—	—	—	—	1	—	—	—	1	—	—	—	—
93-334	00:07	3.549	9.9	*	*	—	—	*	—	—	1	—	—	—	1	—	—	—	—	—	—	—	—	—	—	—	—
93-342	03:04	3.595	8.1	*	*	—	1	*	1	—	2	—	—	—	1	—	—	—	—	—	—	—	—	—	—	—	—
93-350	03:05	3.641	8.0	*	*	—	—	*	—	—	1	—	—	—	—	—	—	—	—	—	—	—	—	—	—	—	—
93-357	20:09	3.683	7.7	*	*	—	—	*	2	—	1	—	—	—	—	—	—	—	—	—	—	—	—	—	—	—	—
94-002	19:45	3.738	10.0	*	*	—	1	*	—	—	—	—	—	—	2	—	—	—	—	—	—	—	—	—	—	—	—
94-014	19.29	3.801	12.0	*	*	—	—	*	1	—	—	—	—	—	3	—	—	—	2	—	—	—	—	—	—	—	—
94-032	20:19	3.894	18.0	*	*	—	1	*	3	—	2	—	—	—	1	—	—	—	—	—	—	—	—	—	—	—	—
94-044	20:20	3.954	12.0	*	*	—	—	*	2	—	1	—	—	—	2	—	—	—	1	—	—	—	—	—	—	—	—
94-055	15:49	4.006	10.8	*	*	—	—	*	1	—	1	—	—	—	—	—	—	—	1	—	—	—	—	—	—	—	—
94-063	19.09	4.045	8.1	*	*	—	—	*	—	—	2	—	—	—	—	—	—	—	—	—	—	—	—	—	—	—	—
94-074	13:14	4.095	10.8	*	*	—	3	*	2	—	1	—	—	—	1	—	—	—	—	—	—	—	—	—	—	—	—
94-085	13:04	4.145	11.0	*	*	—	4	*	1	—	1	—	—	—	—	—	—	—	—	—	—	—	—	—	—	—	—
94-093	13:05	4.181	8.0	*	*	—	—	*	1	—	—	—	—	—	—	—	—	—	—	—	—	—	—	—	—	—	—
94-101	07:04	4.214	7.7	*	*	—	—	*	—	—	—	—	—	—	3	—	—	—	—	—	—	—	—	—	—	—	—
94-109	07:05	4.249	8.0	*	*	—	3	*	—	—	—	—	—	—	3	—	—	—	—	—	—	—	—	—	—	—	—
94-127	04:51	4.323	17.9	*	*	—	2	*	1	—	2	—	—	—	—	—	—	—	—	—	—	—	—	—	—	—	—
94-135	12:44	4.356	8.3	*	*	—	—	*	—	—	1	—	—	—	2	—	—	—	1	—	—	—	—	—	—	—	—
94-142	14:29	4.384	7.1	*	*	—	1	*	—	—	2	—	—	—	—	—	—	—	—	—	—	—	—	—	—	—	—
94-150	06:14	4.414	7.7	*	*	—	—	*	—	—	1	—	—	—	—	—	—	—	—	—	—	—	—	—	—	—	—
94-161	05:13	4.455	11.0	*	*	—	—	*	1	—	—	—	—	—	2	—	—	—	—	—	—	—	—	—	—	—	—
94-169	06:24	4.485	8.0	*	*	—	2	*	—	—	3	—	—	1	—	1	—	—	—	—	—	—	—	—	—	—	—
94-177	12:38	4.515	8.3	*	*	—	16	*	1	—	1	—	—	—	1	—	—	—	—	—	—	—	—	—	—	—	—
94-185	05:39	4.543	7.7	*	*	—	6	*	1	—	—	—	—	—	—	—	—	—	—	—	—	—	—	—	—	—	—
94-195	10:10	4.578	10.2	*	*	—	—	*	1	—	1	—	—	1	—	—	—	—	—	—	—	—	—	—	—	—	—

94-195	14:05	4.579	0.3																						
94-203	07:29	4.605	7.9	*	3	1	—	*	—	—	—	*	—	—	1	*	—	—	—	*	—	—	—	*	—	—	—
94-211	22:29	4.633	8.6	*	—	—	—	*	—	2	2	*	—	—	—	*	—	1	—	*	—	—	—	*	—	—	—
94-219	07:21	4.657	7.4	*	—	—	1	*	—	1	—	*	—	—	—	*	—	—	—	*	—	—	—	*	—	—	—
94-266	05:10	4.798	46.9	*	2	22	3	*	2	4	8	*	—	2	6	*	—	—	2	*	—	—	—	*	—	—	—
94-274	19:29	4.822	8.6	*	—	2	—	*	—	2	3	*	—	—	—	*	—	—	—	*	—	—	—	*	—	—	—
94-284	22:05	4.850	10.1	*	—	2	—	*	—	1	3	*	—	1	—	*	—	—	—	*	—	1	—	*	—	—	—
94-292	06:15	4.869	7.3	*	—	3	—	*	—	1	3	*	—	—	3	*	—	—	—	*	—	—	—	*	—	—	—
94-300	01:45	4.889	7.8	*	—	7	—	*	—	1	—	*	—	—	2	*	—	—	—	*	—	—	—	*	—	—	—
94-309	18.30	4.913	9.7	*	—	7	4	*	—	—	3	*	—	—	—	*	—	—	—	*	—	—	—	*	—	—	—
94-318	19.38	4.935	9.0	*	—	2	1	*	1	1	—	*	—	—	1	*	—	—	1	*	—	—	—	*	—	—	—
94-327	02:13	4.954	8.3	*	—	1	1	*	—	—	1	*	—	—	1	*	—	—	—	*	—	—	—	*	—	—	—
94-343	23:53	4.992	16.9	*	1	5	2	*	1	—	3	*	—	—	2	*	—	—	—	*	—	—	—	*	—	—	—
94-351	03:05	5.007	7.1	*	—	1	—	*	—	—	1	*	—	—	—	*	—	—	1	*	—	—	—	*	—	—	—
94-362	02:45	5.030	11.0	*	1	190	39	*	—	—	2	*	—	—	—	*	—	—	1	*	—	—	—	*	—	—	—
95-007	02:21	5.050	10.0	*	2	142	98	*	—	—	1	*	—	—	—	*	—	—	—	*	—	—	—	*	—	—	—
95-021	21:49	5.078	14.8	*	2	5	—	*	—	—	—	*	—	1	—	*	—	—	—	*	—	—	—	*	—	—	—
95-029	02:18	5.091	7.2	*	1	2	—	*	—	2	1	*	—	—	1	*	—	—	—	*	—	—	—	*	—	—	—
95-044	23:23	5.118	15.9	*	1	17	5	*	—	—	—	*	—	—	1	*	—	—	—	*	—	—	—	*	—	—	—
95-061	20:44	5.145	16.9	*	—	39	10	*	—	2	—	*	—	1	1	*	—	—	—	*	—	—	—	*	—	—	—
95-076	23:08	5.168	15.1	*	—	6	—	*	—	2	4	*	—	1	1	*	—	—	—	*	—	—	—	*	—	—	—
95-086	11:29	5.181	9.5	*	1	470	317	*	—	1	1	*	—	—	—	*	—	—	—	*	—	—	—	*	—	—	—
95-096	17:10	5.194	10.2	*	1	598	292	*	—	4	1	*	—	—	—	*	—	—	—	*	—	—	—	*	—	—	—
95-104	18:28	5.204	8.1	*	2	384	278	*	—	1	1	*	—	—	—	*	—	—	—	*	—	—	—	*	—	—	—
95-113	13:58	5.214	8.8	*	1	7	—	*	—	1	—	*	—	—	1	*	—	—	—	*	—	—	—	*	—	—	—
95-121	12:27	5.223	7.9	*	—	4	2	*	—	—	—	*	—	—	1	*	—	—	—	*	—	—	—	*	—	—	—
95-128	16:24	5.231	7.2	*	—	18	5	*	—	—	—	*	—	—	1	*	—	—	—	*	—	—	—	*	—	—	—
95-138	16:04	5.241	10.0	*	—	8	—	*	—	—	—	*	—	—	—	*	—	—	—	*	—	—	—	*	—	—	—
95-149	16:59	5.251	11.0	*	3	11	—	*	—	1	2	*	—	—	—	*	—	—	—	*	—	—	—	*	—	—	—
95-159	10:28	5.259	9.7	*	—	16	5	*	—	—	—	*	—	—	—	*	—	—	—	*	—	—	—	*	—	—	—
95-166	10:39	5.264	7.0	*	—	8	1	*	—	—	—	*	—	—	—	*	—	—	—	*	—	—	—	*	—	—	—
95-177	12:09	5.272	11.1	*	—	53	10	*	—	—	—	*	—	—	—	*	—	—	—	*	—	—	—	*	—	—	—
95-209	05:59	5.289	31.7	*	—	10#	1#	*	—	2	3	*	—	—	—	*	—	—	—	*	—	—	—	*	—	—	—
95-217	02:31	5.292	7.9	*	—	200#	74#	*	—	1	2	*	—	—	1	*	—	—	—	*	—	—	—	*	—	—	—
95-224	05:17	5.294	7.1	*	—	211#	64#	*	—	5	2	*	—	—	—	*	—	—	—	*	—	—	—	*	—	—	—
95-234	08:39	5.297	10.1	*	—	2#	1#	*	—	4	—	*	—	—	—	*	—	—	1	*	—	—	—	*	—	—	—
95-244	15:44	5.299	10.3	*	—	45#	10#	*	—	5	5	*	—	—	1	*	—	—	—	*	—	—	—	*	—	—	—
95-252	01:36	5.299	7.4	*	—	10#	6#	*	—	1	3	*	—	—	—	*	—	—	—	*	—	—	—	*	—	—	—
95-262	02:07	5.300	10.0	*	—	1#	2#	*	—	1	—	*	—	—	—	*	—	—	—	*	—	—	—	*	—	—	—
95-272	00:56	5.299	10.0	*	—	4#	0#	*	—	1	—	*	—	—	—	*	—	—	—	*	—	—	—	*	—	—	—
95-284	22:28	5.298	12.9	*	—	10#	2#	*	—	1	—	*	—	—	1	*	—	—	—	*	—	—	—	*	—	—	—
95-299	12:48	5.294	14.6	*	1	87	22	*	—	—	3	*	—	—	—	*	—	—	—	*	—	—	—	*	—	—	—
95-323	00:12	5.285	23.5	*	1	100	130	*	1	3	1	*	—	—	—	*	—	—	—	*	—	—	—	*	—	—	—
95-333	00:21	5.280	10.0	*	22	330	293	*	—	1	1	*	—	—	—	*	—	—	1	*	—	—	—	*	—	—	—
95-340	05:37	5.277	7.2	*	264	689	336	*	1	1	1	*	—	—	—	*	—	—	—	*	—	—	—	*	—	—	—
95-341	15:30	5.280	1.4	*	11	40	15	*	52	5	3	*	1	1	1	*	—	—	1	*	—	—	—	*	—	—	—
95-341	17:45	5.281	0.1	*	15	12	1	*	13	7	—	*	1	—	—	*	—	—	—	*	—	—	—	*	—	—	—
95-342	00:11	5.282	0.3	*	86	80	—	*	38	28	—	*	6	3	3	*	4	1	—	*	—	1	1	*	—	1	—
95-362	11:57	5.320	20.5	*	11	9	—	*	53	12	—	*	1	1	—	*	—	—	—	*	1	—	1	*	—	—	—
Impacts (counted)				*	432	3871	2085	*	210	106	116	*	20	14	90	*	12	2	31	*	3	3	8	*	3	1	1
Impacts (complete data)				*	39	847	1244	*	72	68	97	*	12	9	86	*	5	2	30	*	0	2	7	*	3	1	1
All events (complete data)				1533	265	847	1244	127	72	68	97	0	12	9	86	2	5	2	30	0	0	2	7	0	3	1	1

Table 5
DPF data: No., impact time, CLN, AR, SEC, IA, EA, CA, IT, ET, EIT, EIC, ICC, PA, PET, EVD, ICP, ECP, CCP, PCP, HV and evaluated data: R, LON, LAT, D_{Jup}, rotation angle (ROT), instr. pointing (S_{LON}, S_{LAT}), speed (V), speed error factor (*VEF*), mass (V) and mass error factor (*MEF*). For entries with HV = X, the channeltron high voltage was switched off

No.	IMP. DATE	CLN	AR	SEC	IA	EA	CA	IT	ET	EIT	EIC	ICC	PA	PET	EVD	ICP	ECP	CCP	PCP	HV	R	LON	LAT	D_{Jup}	ROT	S_{LON}	S_{LAT}	V	*VEF*	M	*MEF*
360	93-008 14:56	3	2	6	11	22	3	13	10	11	0	1	22	1	1	0	1	0	1	2	1.05141	115.4	−1.0	5.14281	82	199	17	2.3	1.9	$3.7\cdot10^{-10}$	10.5
361	93-009 16:49	3	4	12	25	29	28	11	10	6	0	1	47	0	1	0	1	0	1	2	1.05689	116.6	−1.0	5.12109	73	200	24	5.2	1.9	$4.9\cdot10^{-10}$	10.3
362	93-010 14:24	3	3	217	19	21	17	14	4	15	0	1	17	1	1	0	1	0	1	2	1.06158	117.6	−1.0	5.10304	145	173	−27	11.8	9.5	$5.1\cdot10^{-12}$	2690.1
363	93-010 23:01	3	3	255	23	22	11	3	1	5	0	1	27	0	1	0	1	0	1	2	1.06349	118.0	−1.0	5.09584	91	197	9	70.0	1.9	$1.6\cdot10^{-14}$	10.5
364	93-011 11:58	3	5	197	55	56	31	14	10	5	0	1	47	0	1	0	1	0	1	2	1.06640	118.6	−1.0	5.08505	173	148	−36	2.0	1.9	$7.8\cdot10^{-07}$	10.5
365	93-012 00:54	1	6	0	59	8	31	4	0	4	1	1	31	0	1	0	1	0	1	2	1.06934	119.2	−1.0	5.07428	999	999	999	39.6	1.9	$9.0\cdot10^{-13}$	10.5
366	93-015 23:49	1	2	187	13	13	1	12	15	0	1	1	47	31	1	0	1	0	1	2	1.09216	123.5	−1.1	4.99591	187	134	−36	4.5	1.9	$1.7\cdot10^{-11}$	10.5
367	93-016 12:45	3	2	48	12	20	2	10	3	11	0	1	22	1	1	0	1	0	1	2	1.09543	124.1	−1.1	4.98532	23	185	63	9.7	1.9	$2.9\cdot10^{-12}$	10.5
368	93-016 12:45	3	3	31	22	12	10	5	4	12	0	1	17	1	1	0	1	0	1	2	1.09543	124.1	−1.1	4.98532	46	198	45	29.8	1.9	$1.2\cdot10^{-13}$	10.5
369	93-016 21:23	2	3	49	23	3	11	11	15	8	0	1	47	1	1	0	1	0	1	2	1.09763	124.5	−1.1	4.97827	21	184	64	2.3	1.9	$1.3\cdot10^{-10}$	10.5
370	93-017 10:20	1	2	240	11	0	1	13	0	0	0	1	47	0	1	0	1	0	1	2	1.10096	125.0	−1.2	4.96770	113	191	−6	2.3	1.9	$2.0\cdot10^{-10}$	10.5
371	93-017 10:20	1	4	178	26	30	28	9	9	2	1	1	10	5	1	0	1	0	1	2	1.10096	125.0	−1.2	4.96770	200	122	−33	12.1	1.6	$5.9\cdot10^{-11}$	6.0
372	93-019 01:09	1	2	20	11	9	7	15	15	0	1	1	7	30	1	0	1	0	1	2	1.11117	126.7	−1.2	4.93619	62	200	33	2.0	1.9	$1.2\cdot10^{-10}$	10.5
373	93-020 03:02	1	2	0	11	12	1	12	15	0	1	1	47	31	1	0	1	0	1	2	1.11815	127.8	−1.2	4.91530	999	999	999	4.5	1.9	$1.0\cdot10^{-11}$	10.5
374	93-020 03:02	3	5	0	52	52	31	12	14	13	0	1	47	0	1	0	1	0	1	2	1.11815	127.8	−1.2	4.91530	999	999	999	2.0	1.9	$2.6\cdot10^{-07}$	10.5
376	93-022 02:30	3	3	254	19	23	24	5	4	5	0	1	43	0	1	0	1	0	1	2	1.13129	129.8	−1.2	4.87726	93	189	−6	45.7	1.6	$5.9\cdot10^{-14}$	6.0
377	93-023 08:41	3	2	233	10	23	1	8	8	15	0	1	24	2	1	0	1	0	1	2	1.13986	131.0	−1.2	4.85325	122	187	−30	19.0	1.9	$5.2\cdot10^{-13}$	10.5
378	93-024 23:31	3	4	30	26	49	17	4	4	5	0	1	47	0	1	0	1	0	1	2	1.15113	132.6	−1.3	4.82259	48	176	28	39.6	1.9	$1.5\cdot10^{-12}$	10.5
379	93-027 03:17	1	2	0	12	14	1	13	0	11	0	1	21	1	1	0	1	0	1	2	1.16656	134.6	−1.3	4.78212	999	999	999	2.3	1.9	$1.8\cdot10^{-10}$	10.5
380	93-031 19:27	1	2	135	12	10	9	15	15	0	1	1	6	31	1	0	1	0	1	2	1.20139	138.9	−1.4	4.69604	260	77	−12	2.0	1.9	$1.7\cdot10^{-10}$	10.5
381	93-034 03:32	3	3	194	19	10	11	12	9	15	0	1	9	1	1	0	1	0	1	2	1.21946	140.9	−1.4	4.65385	177	138	−62	2.0	1.9	$4.1\cdot10^{-10}$	10.5
382	93-037 04:53	1	2	25	12	6	11	13	0	10	0	1	13	1	1	0	1	0	1	2	1.24368	143.5	−1.4	4.59957	55	180	23	2.3	1.9	$4.8\cdot10^{-11}$	10.5
383	93-040 10:32	3	2	20	12	20	1	9	14	15	0	1	24	0	1	0	1	0	1	2	1.26996	146.1	−1.4	4.54320	62	215	24	12.7	1.9	$1.5\cdot10^{-12}$	10.5
384	93-042 22:56	3	2	138	11	9	1	15	4	13	0	1	17	1	1	0	1	0	1	2	1.29081	148.0	−1.4	4.50016	256	109	−10	2.0	1.9	$1.2\cdot10^{-10}$	10.5
386	93-045 02:42	3	5	201	49	53	21	7	6	5	0	1	47	0	1	0	1	0	1	2	1.30894	149.6	−1.5	4.46382	167	180	−50	36.7	2.0	$1.1\cdot10^{-11}$	12.5
388	93-047 19:24	1	6	223	57	12	30	13	0	4	0	1	31	0	1	0	1	0	1	2	1.33190	151.6	−1.5	4.41912	136	207	−34	2.0	1.9	$1.8\cdot10^{-08}$	10.5
389	93-048 12:40	3	5	65	52	49	17	15	15	6	0	1	30	0	1	0	1	0	1	2	1.33807	152.1	−1.5	4.40733	359	161	57	2.0	1.9	$1.5\cdot10^{-07}$	10.5
390	93-050 03:29	1	4	197	26	30	26	9	7	0	1	1	8	3	1	0	1	0	1	2	1.35203	153.2	−1.5	4.38102	173	173	−52	15.0	1.7	$3.4\cdot10^{-11}$	7.1
391	93-051 01:04	1	3	229	21	21	9	7	9	0	1	1	47	31	1	0	1	0	1	2	1.35983	153.8	−1.5	4.36652	128	211	−28	12.7	1.9	$5.4\cdot10^{-12}$	10.5
392	93-051 18:19	3	3	252	21	25	3	5	6	7	0	1	46	0	1	0	1	0	1	2	1.36609	154.3	−1.5	4.35499	96	218	−3	33.1	1.6	$3.9\cdot10^{-13}$	6.0
393	93-052 02:57	3	3	253	20	24	25	12	12	7	0	1	43	0	1	0	1	0	1	2	1.36923	154.6	−1.5	4.34924	94	218	−1	2.5	1.6	$1.1\cdot10^{-09}$	6.0
395	93-054 02:24	1	2	101	12	12	1	13	14	0	1	1	47	31	1	0	1	0	1	2	1.38655	155.9	−1.5	4.31790	308	114	31	2.3	1.9	$1.3\cdot10^{-10}$	10.5
396	93-054 23:58	3	3	31	19	24	13	7	8	6	0	1	43	0	1	0	1	0	1	2	1.39447	156.5	−1.5	4.30379	46	210	36	18.3	1.6	$2.3\cdot10^{-12}$	6.0
397	93-055 17:13	1	2	172	10	13	7	15	14	0	1	1	47	17	1	0	1	0	1	2	1.40082	157.0	−1.5	4.29257	208	130	−44	2.5	1.6	$7.4\cdot10^{-11}$	6.0
398	93-057 03:44	3	2	131	12	20	2	10	3	11	0	1	24	1	1	0	1	0	1	2	1.41356	157.6	−1.5	4.27029	266	108	−1	9.7	1.9	$2.9\cdot10^{-12}$	10.5
399	93-059 03:12	3	4	6	25	25	17	8	3	15	0	1	24	0	1	0	1	0	1	2	1.43116	159.1	−1.5	4.24000	82	218	8	9.7	1.9	$4.0\cdot10^{-11}$	10.5
401	93-063 23:40	1	2	207	13	13	1	14	15	0	1	1	47	31	1	0	1	0	1	2	1.47471	162.0	−1.5	4.16744	159	190	−48	2.0	1.9	$3.3\cdot10^{-10}$	10.5
403	93-067 01:01	3	3	18	23	29	28	9	6	5	0	1	47	0	1	0	1	0	1	2	1.50235	163.8	−1.5	4.12299	65	216	21	16.3	1.9	$1.5\cdot10^{-11}$	10.1
404	93-068 07:13	3	2	254	13	21	17	14	15	8	0	1	9	14	1	0	1	0	1	2	1.51377	164.5	−1.5	4.10496	93	218	0	2.0	1.9	$8.1\cdot10^{-10}$	10.5
405	93-068 11:31	3	2	228	12	3	1	11	15	15	0	1	6	7	1	0	1	0	1	2	1.51540	164.6	−1.5	4.10241	129	210	−29	7.2	1.9	$6.5\cdot10^{-13}$	10.5
406	93-070 02:21	1	4	0	28	29	25	13	13	0	1	1	27	15	1	0	1	0	1	2	1.53012	165.5	−1.5	4.07949	999	999	999	2.0	1.9	$2.3\cdot10^{-08}$	10.5
407	93-070 02:21	3	5	0	50	55	21	14	4	5	0	1	63	0	1	0	1	0	1	2	1.53012	165.5	−1.5	4.07949	999	999	999	11.8	9.5	$9.3\cdot10^{-10}$	2690.1
408	93-071 04:14	3	2	0	8	22	1	15	13	15	0	1	23	3	1	0	1	0	1	2	1.53994	166.1	−1.5	4.06436	999	999	999	2.0	1.9	$4.2\cdot10^{-10}$	10.5
409	93-074 01:16	3	2	25	8	11	17	11	13	12	0	1	3	7	1	0	1	0	1	2	1.56619	167.6	−1.5	4.02457	55	213	29	74	1.6	$1.1\cdot10^{-12}$	6.0
411	93-080 21:12	1	4	28	28	7	19	5	0	8	0	1	12	1	1	0	1	0	1	2	1.62872	171.0	−1.5	3.93323	51	212	32	29.8	1.9	$1.3\cdot10^{-13}$	10.5
412	93-081 14:27	1	2	218	11	3	1	8	1	0	1	1	20	11	1	0	1	0	1	2	1.63531	171.3	−1.5	3.92388	143	203	−39	19.0	1.9	$3.5\cdot10^{-14}$	10.5
413	93-082 16:20	3	4	64	24	30	11	6	4	5	0	1	47	0	1	0	1	0	1	2	1.64520	171.8	−1.5	3.90992	0	163	56	36.5	1.6	$9.8\cdot10^{-13}$	6.0
416	93-096 08:12	3	2	174	11	6	1	11	5	14	0	1	14	3	1	0	1	0	1	2	1.77030	177.8	−1.5	3.74201	205	132	−46	7.2	1.9	$8.8\cdot10^{-13}$	10.5
417	93-097 10:05	3	3	0	23	28	17	7	6	6	0	1	47	0	1	0	1	0	1	2	1.78014	178.2	−1.5	3.72942	999	999	999	21.6	1.6	$4.1\cdot10^{-12}$	6.0
418	93-100 15:45	1	6	218	59	61	31	9	7	0	1	1	31	3	1	0	1	0	1	2	1.80962	179.5	−1.5	3.69220	143	203	−39	15.0	1.7	$2.0\cdot10^{-08}$	7.1

419	93-103 12.46	1	2	60	13	12	2	10	15	0	1	1	11	31	1	0	1	0	1	2	1.83575	180.6	−1.5	3.65982	6	171	55	9.7	1.9	$1.4\cdot10^{-12}$	10.5
420	93-104 06:01	3	2	239	11	10	7	14	5	14	0	1	47	2	1	0	1	0	1	2	1.84228	180.9	−1.5	3.65183	114	215	−18	2.0	1.9	$1.4\cdot10^{-10}$	10.5
421	93-104 06:01	3	3	75	21	25	1	9	5	7	0	1	47	0	1	0	1	0	1	2	1.84228	180.9	−1.5	3.65183	345	141	53	20.1	2.6	$2.4\cdot10^{-12}$	28.8
422	93-107 15.59	3	6	159	57	57	31	15	15	11	0	1	25	2	1	0	1	0	1	2	1.87320	182.1	−1.5	3.61437	226	117	−33	2.0	1.9	$1.4\cdot10^{-06}$	10.5
423	93-108 09:15	3	3	232	21	26	7	4	4	5	0	1	46	0	1	0	1	0	1	2	1.87969	182.4	−1.5	3.60659	124	212	−26	52.6	1.6	$6.8\cdot10^{-14}$	6.0
424	93-108 22:11	3	3	59	20	7	8	7	15	6	0	1	59	1	1	0	1	0	1	2	1.88456	182.6	−1.5	3.60079	7	173	55	12.7	1.9	$7.3\cdot10^{-13}$	10.5
425	93-109 15:27	1	2	186	15	8	6	13	0	7	0	1	49	2	1	0	1	0	1	2	1.89105	182.8	−1.5	3.59307	188	151	−52	2.3	1.9	$1.0\cdot10^{-10}$	10.5
426	93-114 16:14	3	4	243	24	31	20	7	3	5	0	1	47	0	1	0	1	0	1	2	1.93630	184.6	−1.4	3.54015	108	216	−14	12.7	1.9	$4.4\cdot10^{-11}$	10.5
427	93-114 20:33	1	3	9	19	14	5	9	15	0	1	1	47	31	1	0	1	0	1	2	1.93791	184.6	−1.4	3.53829	77	217	11	7.2	1.9	$9.2\cdot10^{-12}$	10.5
428	93-116 15:42	1	3	210	19	8	6	14	9	0	1	1	6	23	1	0	1	0	1	2	1.95400	185.2	−1.4	3.51984	155	194	−46	2.0	1.9	$2.9\cdot10^{-10}$	10.5
429	93-117 04:38	1	2	229	11	10	2	8	15	0	1	1	47	31	1	0	1	0	1	2	1.95882	185.4	−1.4	3.51435	128	211	−29	19.0	1.9	$1.1\cdot10^{-13}$	10.5
430	93-120 05:59	3	3	4	20	25	12	5	6	6	0	1	45	0	1	0	1	0	1	2	1.98607	186.4	−1.4	3.48360	84	218	5	33.1	1.6	$3.4\cdot10^{-13}$	6.0
431	93-122 05:26	3	2	227	8	21	1	4	14	15	0	1	23	3	1	0	1	0	1	2	2.00363	187.0	−1.4	3.46403	131	210	−31	70.0	1.9	$1.7\cdot10^{-15}$	10.5
432	93-126 08:39	3	2	121	15	20	7	12	6	15	0	1	19	1	1	0	1	0	1	2	2.04020	188.3	−1.4	3.42394	280	114	8	12.9	2.7	$2.3\cdot10^{-12}$	32.7
433	93-126 12:58	3	2	5	10	13	2	13	3	14	0	1	18	2	1	0	1	0	1	2	2.04179	188.4	−1.4	3.42222	83	223	5	12.7	8.3	$5.3\cdot10^{-13}$	1706.8
434	93-129 05:41	3	3	215	21	24	17	6	10	6	0	1	42	0	1	0	1	0	1	2	2.06551	189.2	−1.4	3.39668	148	206	−43	15.0	1.6	$6.0\cdot10^{-12}$	6.0
435	93-131 09:27	3	3	18	21	26	13	6	6	6	0	1	46	0	1	0	1	0	1	2	2.08441	189.8	−1.4	3.37657	65	220	20	26.4	1.6	$9.5\cdot10^{-13}$	6.0
436	93-132 19:58	1	2	93	14	15	2	14	15	0	1	1	47	31	1	0	1	0	1	2	2.09698	190.2	−1.4	3.36332	319	126	38	2.0	1.9	$5.1\cdot10^{-10}$	10.5
438	93-137 20:45	3	2	127	9	20	1	12	3	12	0	1	19	1	1	0	1	0	1	2	2.14074	191.7	−1.4	3.31791	271	113	1	4.5	1.9	$1.8\cdot10^{-11}$	10.5
439	93-140 04:50	3	4	16	24	30	21	8	5	5	0	1	47	0	1	0	1	0	1	2	2.16093	192.3	−1.4	3.29731	68	221	18	23.3	2.0	$4.5\cdot10^{-12}$	13.5
441	93-143 01:52	1	3	155	19	14	12	8	13	0	1	1	47	17	1	0	1	0	1	2	2.18566	193.1	−1.4	3.27238	232	120	−30	9.7	1.9	$3.9\cdot10^{-12}$	10.5
442	93-144 12:23	3	3	72	20	12	6	14	1	8	0	1	8	0	1	0	1	0	1	2	2.19799	193.4	−1.3	3.26009	349	153	52	2.0	1.9	$6.1\cdot10^{-10}$	10.5
443	93-146 16:09	1	2	165	12	19	3	15	13	0	1	1	45	27	1	0	1	0	1	2	2.21641	194.0	−1.3	3.24186	218	126	−40	2.0	1.9	$4.8\cdot10^{-10}$	10.5
444	93-148 02:39	3	3	34	20	25	19	11	10	6	0	1	10	0	1	0	1	0	1	2	2.22865	194.4	−1.3	3.22984	42	212	37	5.2	1.9	$1.2\cdot10^{-10}$	10.3
445	93-154 01:01	3	3	240	23	29	14	6	5	5	0	1	47	0	1	0	1	0	1	2	2.27883	195.9	−1.3	3.18139	113	222	−18	32.6	1.6	$1.1\cdot10^{-12}$	6.0
446	93-155 07:13	3	3	0	19	24	13	7	8	6	0	1	44	0	1	0	1	0	1	2	2.28940	196.2	−1.3	3.17134	999	999	999	18.3	1.6	$2.3\cdot10^{-12}$	6.0
447	93-157 15:18	3	2	23	13	9	1	14	3	13	0	1	56	2	1	0	1	0	1	2	2.30897	196.7	−1.3	3.15288	58	218	25	2.0	1.9	$1.7\cdot10^{-10}$	10.5
448	93-167 03:57	3	3	30	22	27	27	4	4	5	0	1	47	14	3	0	1	0	1	2	2.38786	198.9	−1.3	3.08029	48	214	32	52.6	1.6	$9.8\cdot10^{-14}$	6.0
449	93-169 20:40	3	4	21	26	49	11	6	15	5	0	1	47	0	1	0	1	0	1	2	2.40993	199.5	−1.3	3.06049	60	219	23	19.0	1.9	$2.4\cdot10^{-11}$	10.5
450	93-173 15:15	3	4	238	25	31	11	6	4	5	0	1	47	0	1	0	1	0	1	2	2.44063	200.3	−1.3	3.03330	115	229	−21	19.0	1.9	$1.5\cdot10^{-11}$	10.5
451	93-181 00:08	3	3	9	21	26	10	4	5	5	0	1	46	0	1	0	1	0	1	2	2.49991	201.9	−1.2	2.98193	77	230	9	47.1	1.6	$1.1\cdot10^{-13}$	6.0
452	93-181 13:04	1	2	70	9	12	5	14	15	0	1	1	3	31	1	0	1	0	1	2	2.50422	202.0	−1.2	2.97826	352	165	51	2.1	1.6	$1.1\cdot10^{-10}$	6.0
453	93-185 20:37	3	3	8	20	25	20	9	9	6	0	1	44	0	1	0	1	0	1	2	2.53848	202.8	−1.2	2.94928	79	230	7	12.1	1.6	$1.1\cdot10^{-11}$	6.0
454	93-187 20:04	1	2	10	15	7	10	10	14	0	1	1	8	16	1	0	1	0	1	2	2.55408	203.2	−1.2	2.93623	76	230	10	9.7	1.9	$8.3\cdot10^{-13}$	10.5
455	93-189 15:12	3	2	118	11	8	13	14	2	14	0	1	12	1	1	0	1	0	1	2	2.56822	203.6	−1.2	2.92451	284	122	10	2.0	1.9	$1.0\cdot10^{-10}$	10.5
456	93-191 01:43	1	3	171	20	11	7	9	0	11	0	1	18	1	1	0	1	0	1	2	2.57949	203.8	−1.2	2.91521	210	152	−47	7.2	1.9	$6.1\cdot10^{-12}$	10.5
457	93-193 01:10	3	3	98	20	23	6	6	5	6	0	1	43	0	1	0	1	0	1	2	2.59493	204.2	−1.2	2.90254	312	143	31	32.6	1.6	$2.5\cdot10^{-13}$	6.0
458	93-194 03:04	3	4	44	28	50	14	7	12	5	0	1	47	0	1	0	1	0	1	2	2.60332	204.4	−1.2	2.89569	28	221	44	12.7	1.9	$1.6\cdot10^{-10}$	10.5
459	93-196 15:27	1	2	213	10	7	1	9	15	0	1	1	17	31	1	0	1	0	1	2	2.62284	204.9	−1.2	2.87988	150	225	−47	12.7	1.9	$2.0\cdot10^{-13}$	10.5
460	93-197 04:24	3	2	246	15	21	8	10	10	6	0	1	40	0	1	0	1	0	1	2	2.62701	205.0	−1.2	2.87651	104	243	−12	10.7	1.6	$4.3\cdot10^{-12}$	6.0
461	93-197 13:02	1	3	146	23	12	2	15	15	0	1	1	7	29	1	0	1	0	1	2	2.62979	205.1	−1.2	2.87428	245	135	−21	2.0	1.9	$1.0\cdot10^{-09}$	10.5
462	93-202 13:49	1	2	13	14	20	11	10	6	0	1	1	8	8	1	0	1	0	1	2	2.66846	206.0	−1.2	2.84345	72	241	13	18.9	1.6	$6.1\cdot10^{-13}$	6.0
463	93-218 00:50	3	3	29	21	26	7	4	4	5	0	1	46	0	1	0	1	0	1	2	2.78474	208.6	−1.1	2.75385	49	234	30	52.6	1.6	$6.8\cdot10^{-14}$	6.0
464	93-218 18:05	3	4	252	25	31	6	6	4	6	0	1	47	0	1	0	1	0	1	2	2.79006	208.7	−1.1	2.74986	96	244	−5	19.0	1.9	$1.5\cdot10^{-11}$	10.5
465	93-221 15:07	3	2	57	13	19	3	13	10	9	0	1	38	0	1	0	1	0	1	2	2.81125	209.2	−1.1	2.73404	10	201	51	5.2	1.9	$1.9\cdot10^{-11}$	10.3
466	93-223 18:53	1	2	194	9	11	7	12	14	0	1	1	36	18	1	0	1	0	1	2	2.82706	209.5	−1.1	2.72233	177	193	−57	3.8	1.6	$1.1\cdot10^{-11}$	6.0
467	93-226 15:54	3	3	234	22	28	13	4	4	5	0	1	47	0	1	0	1	0	1	2	2.84803	210.0	−1.1	2.70692	121	249	−24	52.6	1.6	$1.2\cdot10^{-13}$	6.0
468	93-227 04:51	3	4	236	25	31	17	6	4	5	0	1	47	0	1	0	1	0	1	2	2.85195	210.1	−1.1	2.70406	118	250	−22	19.0	1.9	$1.5\cdot10^{-11}$	10.5
469	93-227 13:29	3	4	25	29	50	29	5	11	5	0	1	47	0	1	0	1	0	1	2	2.85456	210.1	−1.1	2.70215	55	247	28	29.8	1.9	$9.7\cdot10^{-12}$	10.5
470	93-231 12:23	1	2	251	11	6	1	9	9	0	1	1	22	10	1	0	1	0	1	2	2.88313	210.7	−1.1	2.68142	97	253	−5	12.7	1.9	$2.0\cdot10^{-13}$	10.5
471	93-233 16:09	3	2	51	11	13	8	9	10	5	0	1	0	0	1	0	1	0	1	2	2.89862	211.1	−1.1	2.67028	18	222	50	18.3	1.6	$2.0\cdot10^{-13}$	6.0
472	93-237 10:45	1	3	40	21	22	9	4	10	0	1	1	47	27	1	0	1	0	1	2	2.92555	211.6	−1.1	2.65108	34	236	42	39.6	1.9	$1.1\cdot10^{-13}$	10.5
473	93-241 13:58	3	3	0	22	27	24	4	4	5	0	1	47	0	1	0	1	0	1	2	2.95481	212.2	−1.0	2.63045	999	999	999	52.6	1.6	$9.8\cdot10^{-14}$	6.0
474	93-243 09:07	3	2	32	14	22	21	8	4	6	0	1	42	0	1	0	1	0	1	2	2.96745	212.5	−1.0	2.62161	45	243	35	19.0	1.9	$8.4\cdot10^{-13}$	10.5

continued over

Table 5
Continued

No.	IMP. DATE	CLN	AR	SEC	IA	EA	CA	IT	ET	EIT	EIC	ICC	PA	PET	EVD	ICP	ECP	CCP	PCP	HV	R	LON	LAT	D_{Jup}	ROT	S_{LON}	S_{LAT}	V	VEF	M	MEF
475	93-248 05:36	3	2	249	14	22	5	8	4	6	0	1	42	0	1	0	1	0	1	2	3.00133	213.2	−1.0	2.59811	100	256	−8	19.0	1.9	$8.4\cdot10^{-13}$	10.5
476	93-250 22:18	3	2	30	13	19	11	10	10	7	0	1	36	0	1	0	1	0	1	2	3.02001	213.6	−1.0	2.58529	48	247	33	10.7	1.6	$2.3\cdot10^{-12}$	6.0
477	93-251 19:53	3	3	240	21	26	28	4	4	5	0	1	46	0	1	0	1	0	1	2	3.02621	213.7	−1.0	2.58105	113	254	−18	52.6	1.6	$6.8\cdot10^{-14}$	6.0
478	93-252 08:49	3	4	236	24	29	18	4	4	5	0	1	47	0	1	0	1	0	1	2	3.02993	213.8	−1.0	2.57852	118	253	−22	52.6	1.6	$1.8\cdot10^{-13}$	6.0
479	93-253 06:23	3	3	215	22	27	8	4	5	6	0	1	47	0	1	0	1	0	1	2	3.03611	213.9	−1.0	2.57431	148	239	−43	47.1	1.6	$1.6\cdot10^{-13}$	6.0
480	93-258 15:49	3	2	34	13	21	3	8	4	6	0	1	41	0	1	0	1	0	1	2	3.07296	214.6	−1.0	2.54941	42	250	37	19.0	1.9	$6.1\cdot10^{-13}$	10.5
481	93-259 00:26	3	3	6	20	24	17	6	8	5	0	1	43	0	1	0	1	0	1	2	3.07540	214.7	−1.0	2.54778	82	261	7	22.4	1.6	$1.1\cdot10^{-12}$	6.0
482	93-261 08:31	3	2	15	12	20	7	9	5	6	0	1	39	0	1	0	1	0	1	2	3.09123	215.0	−1.0	2.53720	69	260	17	12.7	1.9	$1.5\cdot10^{-12}$	10.5
483	93-270 12:32	3	2	211	13	19	13	10	8	7	0	1	36	0	1	0	1	0	1	2	3.15256	216.2	−1.0	2.49672	153	239	−46	16.0	1.6	$7.9\cdot10^{-13}$	6.0
484	93-271 05:48	3	3	236	21	26	22	5	5	5	0	1	45	0	1	0	1	0	1	2	3.15732	216.3	−1.0	2.49361	118	258	−22	40.9	1.6	$2.0\cdot10^{-13}$	6.0
485	93-271 05:48	3	3	181	20	20	17	8	4	13	0	1	17	1	1	0	1	0	1	2	3.15732	216.3	−1.0	2.49361	195	186	−51	9.7	1.9	$7.4\cdot10^{-12}$	10.5
486	93-271 14:25	3	3	223	21	25	10	5	7	6	0	1	45	0	1	0	1	0	1	2	3.15970	216.3	−1.0	2.49207	136	251	−35	30.5	1.6	$5.0\cdot10^{-13}$	6.0
487	93-275 04:42	3	4	222	24	29	17	7	5	5	0	1	47	0	1	0	1	0	1	2	3.18337	216.8	−1.0	2.47670	138	250	−36	26.7	1.7	$2.5\cdot10^{-12}$	7.3
488	93-276 02:17	3	3	252	23	29	28	5	5	5	0	1	47	0	1	0	1	0	1	2	3.18926	216.9	−1.0	2.47289	96	256	−4	40.9	1.6	$4.6\cdot10^{-13}$	6.0
489	93-280 05:30	1	2	214	9	10	9	9	10	0	1	1	2	31	1	0	1	0	1	2	3.21622	217.4	−0.9	2.45558	149	237	−43	12.7	1.9	$2.8\cdot10^{-13}$	10.5
491	93-293 21:22	1	2	185	8	4	1	10	15	0	1	1	36	31	1	0	1	0	1	2	3.30369	219.0	−0.9	2.40046	190	188	−53	9.7	1.9	$1.6\cdot10^{-13}$	10.5
492	93-295 03:34	3	4	30	29	52	28	8	5	5	0	1	47	0	1	0	1	0	1	2	3.31162	219.2	−0.9	2.39553	48	248	33	9.7	1.9	$4.3\cdot10^{-10}$	10.5
493	93-298 17:51	1	2	208	8	10	5	12	15	0	1	1	17	31	0	0	1	0	1	2	3.33416	219.6	−0.9	2.38158	158	249	−49	3.2	1.6	$1.4\cdot10^{-11}$	6.0
494	93-301 06:15	1	3	248	23	21	21	10	5	0	1	1	18	11	1	0	1	0	1	2	3.34984	219.9	−0.9	2.37193	101	275	−9	4.5	1.9	$1.6\cdot10^{-10}$	10.5
495	93-301 10:34	3	3	215	21	25	4	4	4	6	0	1	46	0	1	0	1	0	1	2	3.35096	219.9	−0.9	2.37124	148	258	−43	52.6	1.6	$5.7\cdot10^{-14}$	6.0
496	93-304 20:32	3	4	1	25	31	24	8	7	5	0	1	47	0	1	0	1	0	1	2	3.37209	220.3	−0.9	2.35829	89	275	1	9.7	1.9	$9.7\cdot10^{-11}$	10.5
497	93-306 19:59	3	2	226	10	14	22	8	9	6	0	1	36	0	1	0	1	0	1	2	3.38426	220.5	−0.9	2.35087	132	267	−33	24.4	1.6	$6.3\cdot10^{-14}$	6.0
498	93-306 19:59	3	3	46	22	27	12	4	5	5	0	1	47	0	1	0	1	0	1	2	3.38426	220.5	−0.9	2.35087	25	251	47	1.6	47.1	$1.6\cdot10^{-13}$	6.0
500	93-312 05:24	3	3	247	22	27	15	4	5	5	0	1	47	0	1	0	1	0	1	2	3.41717	221.1	−0.9	2.33090	103	275	−10	47.1	1.6	$1.6\cdot10^{-13}$	6.0
501	93-314 00:33	3	4	11	25	31	9	7	4	5	0	1	47	0	1	0	1	0	1	2	3.42806	221.3	−0.9	2.32432	75	274	12	12.7	1.9	$5.2\cdot10^{-11}$	10.5
502	93-315 06:45	3	3	239	22	27	7	4	4	5	0	1	47	0	1	0	1	0	1	2	3.43566	221.4	−0.9	2.31975	114	273	−19	52.6	1.6	$9.8\cdot10^{-14}$	6.0
503	93-320 20:29	1	2	191	12	12	12	11	15	0	1	1	47	31	0	0	1	0	1	2	3.46906	222.0	−0.8	2.29971	181	218	−55	7.2	1.9	$2.8\cdot10^{-12}$	10.5
504	93-323 08:53	3	4	239	30	53	23	8	6	5	0	1	47	0	0	0	0	0	0	2	3.48401	222.3	−0.8	2.29079	114	273	−19	9.7	1.9	$5.9\cdot10^{-10}$	10.5
505	93-323 08:53	3	5	173	52	54	27	15	13	5	0	1	26	0	0	0	0	0	0	2	3.48401	222.3	−0.8	2.29079	207	187	−47	2.5	1.6	$1.3\cdot10^{-07}$	6.0
506	93-326 14:32	3	3	229	21	26	18	7	8	6	0	1	45	0	1	0	1	0	1	3	3.50312	222.6	−0.8	2.27942	128	269	−30	18.3	1.6	$4.1\cdot10^{-12}$	6.0
507	93-333 14:47	3	2	255	8	12	5	9	9	5	0	1	0	0	1	0	1	0	1	2	3.54407	223.3	−0.8	2.25519	91	275	−1	19.9	1.6	$7.4\cdot10^{-14}$	6.0
509	93-334 16:40	3	3	232	19	22	12	8	10	6	0	1	42	0	1	0	1	0	1	2	3.55032	223.4	−0.8	2.25151	124	271	−27	10.7	1.6	$7.5\cdot10^{-12}$	6.0
510	93-335 01:17	3	2	4	11	19	6	9	8	6	0	1	38	0	1	0	1	0	1	2	3.55240	223.5	−0.8	2.25028	84	275	4	12.7	1.9	$1.1\cdot10^{-12}$	10.5
511	93-336 16:07	3	2	2	12	20	12	9	5	8	0	1	39	0	1	0	1	0	1	2	3.56173	223.6	−0.8	2.24479	87	275	2	12.7	1.9	$1.5\cdot10^{-12}$	10.5
512	93-337 05:04	1	2	15	13	4	10	10	15	0	1	1	37	29	1	0	1	0	1	2	3.56483	223.7	−0.8	2.24296	69	288	17	9.7	1.9	$3.8\cdot10^{-13}$	10.5
513	93-342 18:48	3	2	12	15	21	12	10	10	6	0	1	41	0	1	0	1	0	1	2	3.59670	224.2	−0.8	2.22428	73	288	13	10.7	1.6	$4.3\cdot10^{-12}$	6.0
514	93-350 07:59	3	2	43	10	14	5	9	9	7	0	1	36	0	1	0	1	0	1	2	3.63926	225.0	−0.8	2.19944	30	269	45	19.9	1.6	$1.4\cdot10^{-13}$	6.0
515	93-354 06:54	1	2	79	9	3	10	10	15	0	1	1	39	30	1	0	1	0	1	2	3.66129	225.4	−0.8	2.18663	339	208	49	9.7	1.9	$1.7\cdot10^{-13}$	10.5
516	93-356 19:18	1	2	34	9	10	11	11	10	0	1	1	0	0	1	0	1	0	1	3	3.67520	225.6	−0.8	2.17855	42	278	37	7.2	1.9	$1.2\cdot10^{-12}$	10.5
517	93-359 16:19	3	3	7	20	23	13	6	5	5	0	1	43	0	1	0	1	0	1	2	3.69101	225.9	−0.8	2.16938	80	289	8	32.6	1.6	$2.5\cdot10^{-13}$	6.0
518	93-361 11:28	3	3	25	19	23	5	7	8	6	0	1	44	0	1	0	1	0	1	2	3.70084	226.0	−0.8	2.16368	55	284	28	18.3	1.6	$2.0\cdot10^{-12}$	6.0
520	94-004 04:58	1	2	66	8	5	7	10	15	0	1	1	0	0	0	0	1	0	1	2	3.74268	226.7	−0.7	2.13947	357	231	54	9.7	1.9	$1.9\cdot10^{-13}$	10.5
521	94-004 09:17	3	3	7	23	29	28	6	5	5	0	1	47	0	0	0	1	0	1	2	3.74365	226.8	−0.7	2.13891	80	289	8	32.6	1.6	$1.1\cdot10^{-12}$	6.0
522	94-005 15:29	3	4	78	26	49	20	10	15	6	0	1	12	0	0	0	0	0	0	2	3.75039	226.9	−0.7	2.13502	340	209	50	4.5	1.9	$1.7\cdot10^{-09}$	10.5
523	94-009 10:04	3	4	22	24	30	22	6	5	5	0	1	47	0	1	0	1	0	1	2	3.77051	227.2	−0.7	2.12340	59	285	25	32.6	1.6	$1.5\cdot10^{-12}$	6.0
524	94-011 11:56	3	3	0	19	23	17	7	8	6	0	1	43	0	1	0	1	0	1	2	3.77622	227.3	−0.7	2.12010	999	999	999	18.3	1.6	$2.0\cdot10^{-12}$	6.0
525	94-010 11:57	3	3	51	22	26	28	4	4	5	0	1	46	0	1	0	1	0	1	2	3.77622	227.3	−0.7	2.12009	18	258	51	52.6	1.6	$8.4\cdot10^{-14}$	6.0
526	94-015 04:07	3	2	31	12	19	1	8	6	7	0	1	39	0	1	0	1	0	1	2	3.80084	227.7	−0.7	2.10587	46	280	34	19.0	1.9	$3.6\cdot10^{-13}$	10.5
527	94-018 05:28	1	2	247	8	13	1	11	15	0	1	1	59	31	1	0	1	0	1	2	3.81681	228.0	−0.7	2.09665	103	289	−10	4.1	1.6	$1.0\cdot10^{-11}$	6.0
528	94-021 06:48	3	2	251	11	19	1	8	9	7	0	1	38	0	1	0	1	0	1	2	3.83266	228.2	−0.7	2.08749	97	289	−5	19.0	1.9	$3.0\cdot10^{-13}$	10.5
530	94-024 21:05	3	3	1	19	22	7	7	4	5	0	1	42	0	1	0	1	0	1	2	3.85118	228.6	−0.7	2.07679	89	290	1	29.8	2.0	$2.5\cdot10^{-13}$	12.1

531	94-026 16:13	1	2	246	12	15	10	9	9	0	1	1	36	0	1	0	1	0	1	2	3.86038	228.7	−0.7	2.07146	104	289	−11	19.9	1.6	$2.2\cdot10^{-13}$	6.0
532	94-027 05:10	1	2	248	14	13	12	10	15	0	1	1	49	31	1	0	1	0	1	2	3.86313	228.8	−0.7	2.06987	101	289	−8	9.7	1.9	$1.9\cdot10^{-12}$	10.5
533	94-032 23:13	3	2	14	11	19	1	8	7	6	0	1	38	0	1	0	1	0	1	2	3.89231	229.2	−0.7	2.05297	70	288	16	19.0	1.9	$3.0\cdot10^{-13}$	10.5
534	94-040 03:47	3	4	4	27	49	13	5	15	5	0	1	47	0	1	0	1	0	1	2	3.92825	229.8	−0.7	2.03209	84	300	4	29.8	1.9	$5.1\cdot10^{-12}$	10.5
535	94-041 09:59	3	3	19	20	23	4	5	5	6	0	1	43	0	1	0	1	0	1	2	3.93449	229.9	−0.7	2.02846	63	297	21	40.9	1.6	$1.0\cdot10^{-13}$	6.0
536	94-043 09:26	1	2	207	14	14	11	11	10	0	1	1	36	7	1	0	1	0	1	2	3.94424	230.1	−0.7	2.02277	159	272	−49	7.2	1.9	$5.4\cdot10^{-12}$	10.5
537	94-043 22:22	1	2	215	11	5	9	10	15	0	1	1	40	31	1	0	1	0	1	2	3.94690	230.2	−0.7	2.02123	148	283	−43	9.7	1.9	$3.1\cdot10^{-13}$	10.5
538	94-043 22:22	3	3	239	20	24	18	11	10	5	0	1	5	1	1	0	1	0	1	2	3.94690	230.2	−0.7	2.02123	114	298	−19	5.2	1.9	$9.8\cdot10^{-11}$	10.3
539	94-046 19:24	1	2	85	14	12	11	11	15	0	1	1	49	31	1	0	1	0	1	2	3.96100	230.4	−0.7	2.01300	330	210	45	7.2	1.9	$3.9\cdot10^{-12}$	10.5
540	94-048 23:10	3	2	27	12	20	2	9	5	6	0	1	41	0	1	0	1	0	1	2	3.97151	230.6	−0.7	2.00685	52	293	30	12.7	1.9	$1.5\cdot10^{-12}$	10.5
541	94-049 16:25	3	4	218	28	50	14	6	10	5	0	1	47	0	1	0	1	0	1	2	3.97501	230.6	−0.6	2.00480	143	286	−40	19.0	1.9	$4.6\cdot10^{-11}$	10.5
542	94-058 07:30	3	2	160	14	20	6	9	8	10	0	1	37	0	1	0	1	0	1	2	4.01650	231.3	−0.6	1.98043	225	200	−35	18.3	1.6	$6.9\cdot10^{-13}$	6.0
543	94-059 09:23	3	2	21	9	19	1	13	6	8	0	1	47	0	1	0	1	0	1	2	4.02163	231.4	−0.6	1.97740	60	296	24	2.3	1.9	$1.6\cdot10^{-10}$	10.5
544	94-065 20:41	3	2	107	8	12	22	8	8	6	0	1	35	0	1	0	1	0	1	2	4.05215	231.9	−0.6	1.95933	300	194	24	26.4	1.6	$2.5\cdot10^{-14}$	6.0
545	94-065 20:41	3	3	241	20	24	11	5	4	5	0	1	44	0	1	0	1	0	1	2	4.05215	231.9	−0.6	1.95933	111	298	−16	45.7	1.6	$7.8\cdot10^{-14}$	6.0
546	94-067 07:12	1	2	66	9	4	1	11	13	0	1	1	9	21	1	0	1	0	1	2	4.05888	232.0	−0.6	1.95534	357	241	54	7.2	1.9	$4.6\cdot10^{-13}$	10.5
550	94-072 03:41	1	2	213	8	0	8	10	0	0	0	1	35	0	1	0	1	0	1	2	4.08140	232.4	−0.6	1.94190	150	280	−45	9.7	1.9	$6.5\cdot10^{-13}$	10.5
552	94-075 13:39	1	2	70	12	4	6	11	15	0	1	1	8	30	1	0	1	0	1	2	4.09711	232.6	−0.6	1.93249	352	233	54	7.2	1.9	$7.4\cdot10^{-13}$	10.5
554	94-076 02:36	3	2	2	10	19	5	9	8	7	0	1	38	0	1	0	1	0	1	2	4.09957	232.7	−0.6	1.93101	87	300	2	12.7	1.9	$9.1\cdot10^{-13}$	10.5
557	94-090 03:05	1	2	96	13	8	1	10	15	0	1	1	42	31	1	0	1	0	1	2	4.16269	233.7	−0.6	1.89274	315	200	35	9.7	1.9	$7.3\cdot10^{-13}$	10.5
558	94-093 21:41	3	3	186	20	21	11	8	13	5	0	1	41	1	1	0	1	0	1	2	4.17934	234.0	−0.6	1.88252	188	233	−53	9.7	1.9	$9.0\cdot10^{-12}$	10.5
559	94-097 16:17	3	3	6	20	23	10	6	5	6	0	1	43	0	1	0	1	0	1	2	4.19584	234.3	−0.6	1.87233	82	300	7	32.6	1.6	$2.5\cdot10^{-13}$	6.0
560	94-098 18:10	3	3	195	21	25	11	5	7	5	0	1	46	0	1	0	1	0	1	2	4.20053	234.3	−0.6	1.86943	176	251	−54	30.5	1.6	$5.0\cdot10^{-13}$	6.0
563	94-103 06:01	3	3	129	23	26	26	10	11	8	0	1	43	0	1	0	1	0	1	2	4.21994	234.7	−0.5	1.85734	269	190	0	5.9	1.6	$1.6\cdot10^{-10}$	6.0
565	94-105 14:06	3	3	58	19	24	1	7	4	6	0	1	45	0	1	0	1	0	1	2	4.22996	234.8	−0.5	1.85107	8	257	54	29.8	2.0	$3.6\cdot10^{-13}$	12.1
566	94-107 00:37	3	3	241	19	22	5	8	4	6	0	1	43	0	1	0	1	0	1	2	4.23609	234.0	−0.5	1.84722	111	298	−16	26.1	2.4	$4.0\cdot10^{-13}$	23.7
567	94-120 12:10	1	2	235	13	5	11	10	15	0	1	1	37	30	1	0	1	0	1	2	4.29261	235.9	−0.5	1.81124	120	291	−23	9.7	1.9	$4.4\cdot10^{-13}$	10.5
568	94-120 12:10	3	2	215	8	11	1	9	10	8	0	1	0	0	1	0	1	0	1	2	4.29261	235.9	−0.5	1.81124	148	278	−43	18.3	1.6	$8.9\cdot10^{-14}$	6.0
569	94-121 22:41	3	2	6	14	21	7	9	5	7	0	1	41	0	1	0	1	0	1	2	4.29853	236.0	−0.5	1.80742	82	295	7	12.7	1.9	$2.5\cdot10^{-12}$	10.5
572	94-129 07:33	3	3	248	22	27	5	4	4	5	0	1	47	0	1	0	1	0	1	2	4.32856	236.5	−0.5	1.78786	101	295	−8	52.6	1.6	$9.8\cdot10^{-14}$	6.0
573	94-131 02:42	3	3	22	22	27	23	10	9	6	0	1	8	0	1	0	1	0	1	2	4.33581	236.6	−0.5	1.78310	59	291	25	9.5	1.7	$3.6\cdot10^{-11}$	7.6
574	94-131 15:38	3	4	217	24	30	18	4	4	5	0	1	47	0	1	0	1	0	1	2	4.33798	236.6	−0.5	1.78167	145	280	−41	52.6	1.6	$2.1\cdot10^{-13}$	6.0
575	94-133 23:43	3	2	13	10	14	1	8	9	7	0	1	37	0	1	0	1	0	1	2	4.34734	236.8	−0.5	1.77548	72	290	15	24.4	1.6	$6.3\cdot10^{-14}$	6.0
576	94-136 16:26	3	2	5	12	20	1	8	6	6	0	1	39	0	1	0	1	0	1	2	4.35807	237.0	−0.5	1.76835	83	291	6	19.0	1.9	$4.3\cdot10^{-13}$	10.5
578	94-140 02:24	3	2	8	9	14	9	10	10	7	0	1	36	0	1	0	1	0	1	2	4.37157	237.2	−0.5	1.75932	79	291	9	16.0	1.6	$2.8\cdot10^{-13}$	6.0
579	94-149 15:03	3	2	28	10	13	5	9	10	9	0	1	36	0	1	0	1	0	1	2	4.40863	237.8	−0.5	1.73416	51	284	31	18.3	1.6	$1.7\cdot10^{-13}$	6.0
580	94-151 18:49	3	3	234	21	26	8	4	5	5	0	1	46	0	1	0	1	0	1	2	4.41690	238.0	−0.5	1.72847	121	288	−24	47.1	1.6	$1.1\cdot10^{-13}$	6.0
581	94-153 13:57	1	2	208	14	13	4	10	15	0	1	1	60	31	1	0	1	0	1	2	4.42376	238.1	−0.5	1.72373	158	266	−49	9.7	1.9	$1.9\cdot10^{-12}$	10.5
582	94-155 17:44	3	3	46	22	27	19	10	15	5	0	1	44	0	1	0	1	0	1	2	4.43195	238.2	−0.5	1.71804	25	268	47	3.8	1.6	$6.0\cdot10^{-10}$	6.0
584	94-163 02:36	2	3	27	21	25	14	4	5	5	0	1	46	0	1	0	1	0	1	2	4.45961	238.7	−0.4	1.69862	52	280	30	47.1	1.6	$9.2\cdot10^{-14}$	6.0
585	94-165 23:38	3	2	236	8	12	9	8	9	7	0	1	0	0	1	0	1	0	1	2	4.47027	238.9	−0.4	1.69103	118	283	−22	24.4	1.6	$3.2\cdot10^{-14}$	6.0
587	94-167 18:46	3	2	239	11	15	1	8	9	7	0	1	37	0	1	0	1	0	1	2	4.47689	239.0	−0.4	1.68630	114	284	−19	24.4	1.6	$8.2\cdot10^{-14}$	6.0
588	94-168 07:43	3	2	19	9	12	6	9	11	8	0	1	0	0	1	0	1	0	1	2	4.47887	239.0	−0.4	1.68487	63	283	21	16.0	1.6	$2.0\cdot10^{-13}$	6.0
589	94-169 18:13	3	3	213	19	23	22	7	4	5	0	1	43	0	1	0	1	0	1	2	4.48413	239.1	−0.4	1.68108	150	267	−45	29.8	2.0	$3.0\cdot10^{-13}$	12.1
590	94-171 00:25	3	2	17	10	14	7	9	10	8	0	1	37	0	1	0	1	0	1	2	4.48873	239.2	−0.4	1.67777	66	284	19	18.3	1.6	$2.0\cdot10^{-13}$	6.0
592	94-173 04:11	1	2	237	11	11	7	10	10	0	1	1	0	0	1	0	1	0	1	2	4.49657	239.3	−0.4	1.67208	117	284	−21	9.7	1.9	$8.5\cdot10^{-13}$	10.5
614	94-182 08:13	1	2	222	12	10	14	10	11	0	1	1	34	0	1	0	1	0	1	2	4.52942	239.9	−0.4	1.64789	138	276	−37	9.7	1.9	$8.6\cdot10^{-13}$	10.5
615	94-187 00:22	1	2	49	12	12	11	11	15	0	1	1	44	31	1	0	1	0	1	2	4.54587	240.2	−0.4	1.63555	21	258	49	7.2	1.9	$2.8\cdot10^{-12}$	10.5
616	94-188 15:12	3	2	22	9	13	5	8	9	5	0	1	36	0	1	0	1	0	1	2	4.55152	240.3	−0.4	1.63127	59	282	25	24.4	1.6	$4.6\cdot10^{-14}$	6.0
617	94-190 06:02	2	3	19	21	26	15	4	4	5	0	1	46	0	1	0	1	0	1	2	4.55714	240.4	−0.4	1.62699	63	283	21	52.6	1.6	$6.8\cdot10^{-14}$	6.0
619	94-198 21:06	3	3	245	20	23	26	6	4	5	0	1	43	0	1	0	1	0	1	2	4.58674	240.9	−0.4	1.60416	105	286	−12	36.5	1.6	$1.7\cdot10^{-13}$	6.0
622	94-203 13:16	2	2	195	8	12	0	9	9	6	0	0	36	0	1	0	1	0	1	2	4.60249	241.2	−0.4	1.59177	176	238	−54	19.9	1.6	$7.4\cdot10^{-14}$	6.0
623	94-203 17.35	3	2	204	8	12	1	9	9	7	0	1	35	0	1	0	1	0	1	2	4.60310	241.2	−0.4	1.59129	163	254	−51	19.9	1.6	$7.4\cdot10^{-14}$	6.0
624	94-205 12:43	2	2	224	8	5	1	9	15	0	1	1	0	0	1	0	1	0	1	2	4.60910	241.3	−0.4	1.58652	135	277	−35	12.7	1.9	$1.0\cdot10^{-13}$	10.5

continued over

Table 5
Continued

No.	IMP. DATE	CLN	AR	SEC	IA	EA	CA	IT	ET	EIT	EIC	ICC	PA	PET	EVD	ICP	ECP	CCP	PCP	HV	R	LON	LAT	D_{Jup}	ROT	S_{LON}	S_{LAT}	V	VEF	M	MEF
625	94-207 20:48	2	4	255	24	27	27	14	14	0	1	1	61	10	1	0	1	0	1	2	4.61686	241.5	−0.4	1.58031	91	287	0	2.5	1.6	$3.5\cdot10^{-09}$	6.0
626	94-208 14:04	3	2	28	13	20	12	8	5	5	0	1	40	0	1	0	1	0	1	2	4.61924	241.5	−0.4	1.57840	51	279	31	19.0	1.9	$5.1\cdot10^{-13}$	10.5
627	94-212 00:02	2	2	143	13	7	4	10	15	0	1	1	43	30	0	0	0	0	0	2	4.63048	241.7	−0.4	1.56932	249	178	−17	9.7	1.9	$6.3\cdot10^{-13}$	10.5
629	94-219 13:13	2	2	211	13	21	0	8	4	6	0	0	41	0	1	0	1	0	1	2	4.65495	242.1	−0.4	1.54922	153	265	−47	19.0	1.9	$6.1\cdot10^{-13}$	10.5
630	94-220 10:48	2	3	243	19	9	10	8	15	0	1	1	61	31	1	0	1	0	1	2	4.65783	242.2	−0.4	1.54682	108	285	−14	9.7	1.9	$1.7\cdot10^{-12}$	10.5
631	94-221 16:59	3	2	242	10	14	1	9	9	6	0	1	36	0	1	0	1	0	1	2	4.66185	242.3	−0.4	1.54346	110	285	−15	19.9	1.6	$1.4\cdot10^{-13}$	6.0
633	94-229 14:49	3	2	230	12	20	1	9	5	6	0	1	40	0	1	0	1	0	1	2	4.68681	242.7	−0.3	1.52231	127	281	−29	12.7	1.9	$1.5\cdot10^{-12}$	10.5
634	94-232 03:12	3	2	185	12	21	1	9	4	6	0	1	41	0	1	0	1	0	1	2	4.69463	242.9	−0.3	1.51557	190	218	−53	12.7	1.9	$1.8\cdot10^{-12}$	10.5
635	94-233 18:02	1	2	3	8	6	0	11	12	0	1	0	30	17	1	0	1	0	1	2	4.69964	243.0	−0.3	1.51123	86	286	3	7.2	1.9	$5.4\cdot10^{-13}$	10.5
636	94-233 22:21	1	2	248	14	21	0	9	15	0	1	0	41	31	1	0	1	0	1	2	4.70019	243.0	−0.3	1.51075	101	286	−9	12.7	1.9	$2.5\cdot10^{-12}$	10.5
637	94-236 10:45	3	3	217	21	27	13	4	4	5	0	1	47	0	1	0	1	0	1	2	4.70792	243.1	−0.3	1.50399	145	271	−42	52.6	1.6	$7.9\cdot10^{-14}$	6.0
638	94-238 18:50	2	3	151	19	19	14	10	7	0	1	1	39	7	1	0	1	0	1	2	4.71505	243.3	−0.3	1.49771	238	181	−25	4.5	1.9	$5.9\cdot10^{-11}$	10.5
639	94-238 23:08	3	2	52	13	20	1	8	5	6	0	1	40	0	1	0	1	0	1	2	4.71560	243.3	−0.3	1.49723	17	254	51	19.0	1.9	$5.1\cdot10^{-13}$	10.5
640	94-240 22:36	3	3	0	20	23	26	6	4	6	0	1	43	0	1	0	1	0	1	2	4.72159	243.4	−0.3	1.49191	999	999	999	36.5	1.6	$1.7\cdot10^{-13}$	6.0
641	94-241 02:55	3	3	34	20	25	20	5	6	5	0	1	45	0	1	0	1	0	1	2	4.72214	243.4	−0.3	1.49142	42	275	37	33.1	1.6	$3.4\cdot10^{-13}$	6.0
642	94-242 09:07	2	2	31	8	12	0	9	9	7	0	0	0	0	1	0	1	0	1	2	4.72593	243.5	−0.3	1.48803	46	277	34	19.9	1.6	$7.4\cdot10^{-14}$	6.0
644	94-247 09:54	3	4	168	27	23	17	12	3	13	0	1	29	1	1	0	1	0	1	2	4.74098	243.7	−0.3	1.47446	214	193	−42	2.0	1.9	$7.7\cdot10^{-09}$	10.5
645	94-248 11:47	2	2	170	10	12	1	10	15	0	1	1	18	31	1	0	1	0	1	2	4.74417	243.8	−0.3	1.47155	211	195	−44	4.7	1.7	$7.6\cdot10^{-12}$	6.7
646	94-249 22:18	3	2	0	15	22	1	8	4	6	0	1	43	0	1	0	1	0	1	2	4.74842	243.9	−0.3	1.46766	999	999	999	19.0	1.9	$9.4\cdot10^{-13}$	10.5
647	94-250 02:37	3	3	232	20	23	9	6	8	6	0	1	43	0	1	0	1	0	1	2	4.74895	243.9	−0.3	1.46717	124	282	−27	22.4	1.6	$9.0\cdot10^{-13}$	6.0
649	94-256 09:36	3	4	65	26	49	23	8	15	5	0	1	47	0	1	0	1	0	1	2	4.76730	244.3	−0.3	1.45013	359	230	54	9.7	1.9	$1.6\cdot10^{-10}$	10.5
650	94-257 02:52	3	2	225	12	20	1	9	5	7	0	1	39	0	1	0	1	0	1	2	4.76938	244.3	−0.3	1.44818	134	278	−34	12.7	1.9	$1.5\cdot10^{-12}$	10.5
651	94-257 15:48	3	3	33	20	23	11	7	9	6	0	1	43	0	1	0	1	0	1	2	4.77093	244.3	−0.3	1.44672	44	276	35	16.0	1.6	$3.5\cdot10^{-12}$	6.0
652	94-258 00:26	2	2	227	8	6	5	9	13	0	1	1	0	0	1	0	1	0	1	2	4.77197	244.3	−0.3	1.44574	131	279	−32	12.7	1.9	$1.2\cdot10^{-13}$	10.5
661	94-259 15:16	3	2	95	13	21	10	8	4	5	0	1	40	0	1	0	1	0	1	2	4.77661	244.4	−0.3	1.44134	316	187	36	19.0	1.9	$6.1\cdot10^{-13}$	10.5
662	94-267 04:27	2	2	225	11	9	7	9	11	0	1	1	0	0	1	0	1	0	1	2	4.79799	244.8	−0.3	1.42079	134	278	−34	12.7	1.9	$3.3\cdot10^{-13}$	10.5
663	94-267 13:05	3	2	1	13	20	6	8	5	6	0	1	39	0	1	0	1	0	1	2	4.79900	244.9	−0.3	1.41980	89	287	1	19.0	1.9	$5.1\cdot10^{-13}$	10.5
665	94-269 08:13	3	2	17	10	13	12	10	11	9	0	1	0	0	1	0	1	0	1	2	4.80401	245.0	−0.3	1.41490	66	284	19	14.0	1.6	$4.2\cdot10^{-13}$	6.0
667	94-271 16:18	2	2	238	9	13	7	12	15	0	1	1	61	31	1	0	1	0	1	2	4.81049	245.1	−0.3	1.40851	115	290	−20	3.2	1.6	$2.6\cdot10^{-11}$	6.0
668	94-272 13:52	3	2	1	12	20	8	10	7	7	0	1	39	0	1	0	1	0	1	2	4.81297	245.1	−0.3	1.40605	89	292	1	9.7	1.9	$2.9\cdot10^{-12}$	10.5
669	94-277 01:43	2	5	70	49	51	26	7	5	4	1	1	18	1	1	0	1	0	1	2	4.82526	245.4	−0.3	1.39373	352	226	54	56.0	2.0	$1.5\cdot10^{-12}$	12.5
671	94-277 06:02	2	2	152	9	8	11	12	15	0	1	1	43	31	1	0	1	0	1	2	4.82575	245.4	−0.3	1.39324	236	187	−26	4.5	1.9	$4.0\cdot10^{-12}$	10.5
672	94-278 12:14	2	3	40	21	14	10	10	15	0	1	1	62	31	1	0	1	0	1	2	4.82916	245.5	−0.3	1.38978	34	276	43	4.5	1.9	$5.1\cdot10^{-11}$	10.5
673	94-280 16:00	3	2	21	11	20	5	9	5	8	0	1	41	0	1	0	1	0	1	2	4.83498	245.6	−0.3	1.38385	60	288	24	12.7	1.9	$1.3\cdot10^{-12}$	10.5
675	94-282 11:09	3	2	211	13	22	4	9	4	6	0	1	42	0	1	0	1	0	1	2	4.83980	245.7	−0.3	1.37891	153	270	−46	12.7	1.9	$2.5\cdot10^{-12}$	10.5
676	94-282 15:28	3	2	221	13	20	7	10	8	9	0	1	38	0	1	0	1	0	1	2	4.84028	245.7	−0.3	1.37841	139	280	−38	9.7	1.9	$3.4\cdot10^{-12}$	10.5
678	94-285 16:48	3	2	24	13	20	12	10	6	7	0	1	38	0	1	0	1	0	1	2	4.84840	245.9	−0.3	1.36999	56	287	27	9.7	1.9	$3.4\cdot10^{-12}$	10.5
679	94-286 14:22	3	3	22	20	25	1	5	4	6	0	1	46	0	1	0	1	0	1	2	4.85077	245.9	−0.3	1.36751	59	288	25	45.7	1.6	$9.2\cdot10^{-14}$	6.0
680	94-287 11:56	2	2	235	14	9	17	11	15	0	1	1	39	30	1	0	1	0	1	2	4.85314	246.0	−0.3	1.36503	120	289	−23	7.2	1.9	$2.4\cdot10^{-12}$	10.5
681	94-288 13:50	3	2	15	14	22	12	9	5	6	0	1	42	0	1	0	1	0	1	2	4.85598	246.0	−0.3	1.36205	69	290	17	12.7	1.9	$3.0\cdot10^{-12}$	10.5
683	94-289 15:43	3	2	19	9	13	6	8	9	7	0	1	36	0	1	0	1	0	1	2	4.85880	246.1	−0.3	1.35907	63	289	21	24.4	1.6	$4.6\cdot10^{-14}$	6.0
684	94-291 06:32	3	3	52	20	23	7	6	5	6	0	1	44	0	1	0	1	0	1	2	4.86301	246.2	−0.3	1.35459	17	260	51	32.6	1.6	$2.5\cdot10^{-13}$	6.0
685	94-291 15:10	3	3	253	20	25	6	5	5	5	0	1	46	0	1	0	1	0	1	2	4.86395	246.2	−0.3	1.35360	94	292	−3	40.9	1.6	$1.5\cdot10^{-13}$	6.0
687	94-292 21:22	3	3	240	19	22	4	9	4	6	0	1	42	0	1	0	1	0	1	2	4.86721	246.2	−0.3	1.35011	113	290	−17	22.4	3.1	$6.9\cdot10^{-13}$	52.8
688	94-295 18:23	2	2	47	8	12	1	14	15	0	1	1	23	31	1	0	1	0	1	2	4.87461	246.4	−0.2	1.34214	24	267	48	2.1	1.6	$9.0\cdot10^{-11}$	6.0
694	94-299 08:40	3	3	42	20	23	20	9	11	7	0	1	41	0	1	0	1	0	1	2	4.88377	246.6	−0.2	1.33215	31	273	44	7.4	1.6	$2.6\cdot10^{-11}$	6.0
696	94-300 10:33	3	2	252	10	14	12	9	10	6	0	1	36	0	1	0	1	0	1	2	4.88650	246.6	−0.2	1.32914	96	292	−4	18.3	1.6	$2.0\cdot10^{-13}$	6.0
699	94-301 03:49	3	2	205	8	12	4	9	9	7	0	1	0	0	1	0	1	0	1	2	4.88831	246.7	−0.2	1.32714	162	262	−50	19.9	1.6	$7.4\cdot10^{-14}$	6.0
705	94-306 21:52	3	2	205	10	13	1	8	9	8	0	1	0	0	0	0	1	0	1	2	4.90267	247.0	−0.2	1.31109	162	262	−50	24.4	1.6	$5.3\cdot10^{-14}$	6.0
710	94-311 14.02	1	2	186	9	7	0	12	15	0	1	0	45	31	0	0	0	0	0	2	4.91413	247.2	−0.2	1.29801	188	225	−53	4.5	1.9	$3.4\cdot10^{-12}$	10.5
713	94-315 00:00	2	2	0	11	4	0	7	0	10	0	0	2	31	1	0	1	0	1	2	4.92239	247.4	−0.2	1.28842	999	999	999	29.8	1.9	$7.2\cdot10^{-15}$	10.5

715	94-316 19:08	3	4	66	26	49	23	7	15	5	0	1	47	0	1	0	1	0	1	2	4.92670	247.5	−0.2	1.28337	357	233	55	12.7	1.9	$8.6\cdot10^{-11}$	10.5
716	94-317 03:46	3	3	20	20	24	10	5	5	5	0	1	45	0	1	0	1	0	1	2	4.92756	247.5	−0.2	1.28236	62	289	22	40.9	1.6	$1.2\cdot10^{-13}$	6.0
719	94-325 05:54	3	3	242	19	22	6	8	5	6	0	1	42	0	1	0	1	0	1	2	4.94662	247.9	−0.2	1.25954	110	302	−15	23.3	2.0	$5.9\cdot10^{-13}$	13.5
720	94-325 14:31	3	2	221	8	13	1	9	9	8	0	1	35	0	1	0	1	0	1	2	4.94746	248.0	−0.2	1.25853	139	292	−38	19.9	1.6	$8.7\cdot10^{-14}$	6.0
725	94-334 18:32	3	2	219	12	20	3	9	5	7	0	1	40	0	1	0	1	0	1	2	4.96839	248.4	−0.2	1.23251	142	291	−40	12.7	1.9	$1.5\cdot10^{-12}$	10.5
728	94-339 02:05	1	2	169	11	9	0	11	15	0	1	0	25	31	1	0	1	0	1	2	4.97801	248.6	−0.2	1.22021	212	211	−43	7.2	1.9	$1.4\cdot10^{-12}$	10.5
729	94-340 12:35	3	2	236	10	14	8	11	13	13	0	1	13	1	1	0	1	0	1	2	4.98118	248.7	−0.2	1.21611	118	301	−22	7.4	1.6	$2.5\cdot10^{-12}$	6.0
730	94-341 01:32	3	3	95	22	27	24	4	5	5	0	1	47	0	1	0	1	0	1	2	4.98237	248.7	−0.2	1.21457	316	205	36	47.1	1.6	$1.6\cdot10^{-13}$	6.0
731	94-341 14:29	3	3	37	21	26	11	5	6	5	0	1	46	0	1	0	1	0	1	2	4.98355	248.8	−0.2	1.21302	38	290	40	33.1	1.6	$4.5\cdot10^{-13}$	6.0
732	94-342 07:44	3	2	44	13	20	1	10	7	8	0	1	37	0	1	0	1	0	1	2	4.98513	248.8	−0.2	1.21097	28	283	46	9.7	1.9	$3.4\cdot10^{-12}$	10.5
735	94-346 10:57	3	2	218	10	14	1	8	9	7	0	1	37	0	1	0	1	0	1	2	4.99410	249.0	−0.2	1.19913	143	290	−40	24.4	1.6	$6.3\cdot10^{-14}$	6.0
737	94-350 05:33	3	4	77	24	30	8	5	3	5	0	1	47	0	1	0	1	0	1	2	5.00218	249.2	−0.2	1.18828	342	225	51	45.7	1.6	$3.8\cdot10^{-13}$	6.0
739	94-351 11:45	3	2	5	11	19	8	9	7	6	0	1	37	0	1	0	1	0	1	2	5.00484	249.3	−0.2	1.18466	83	304	6	12.7	1.9	$1.1\cdot10^{-12}$	10.5
740	94-352 05:00	3	2	28	14	22	3	9	4	6	0	1	42	0	1	0	1	0	1	2	5.00636	249.3	−0.2	1.18260	51	297	31	12.7	1.9	$3.0\cdot10^{-12}$	10.5
746	94-359 00:56	3	4	17	24	30	14	6	4	5	0	1	47	0	1	0	1	0	1	2	5.02058	249.7	−0.2	1.16288	66	301	19	36.5	1.6	$9.8\cdot10^{-12}$	6.0
823	95-003 00:39	3	2	237	8	12	7	8	9	6	0	1	0	0	1	0	1	0	1	2	5.03873	250.1	−0.1	1.13680	117	301	−21	24.4	1.6	$3.2\cdot10^{-14}$	6.0
831	95-014 08:26	2	3	183	19	13	5	8	15	0	1	1	47	31	1	0	1	0	1	2	5.06069	250.7	−0.1	1.10372	193	244	−52	9.7	1.9	$3.3\cdot10^{-12}$	10.5
836	95-022 10:34	3	3	53	19	23	10	7	5	6	0	1	43	0	0	0	0	0	0	2	5.07577	251.1	−0.1	1.07994	15	282	−52	26.7	1.7	$4.4\cdot10^{-13}$	7.3
839	95-024 14:20	2	2	171	10	6	8	11	15	0	1	1	45	30	0	0	0	0	0	2	5.07971	251.2	−0.1	1.07358	210	226	−45	7.2	1.9	$7.5\cdot10^{-13}$	10.5
840	95-025 07:35	2	2	217	12	20	0	8	5	6	0	0	40	0	1	0	1	0	1	2	5.08101	251.2	−0.1	1.07146	145	301	−41	19.0	1.9	$4.3\cdot10^{-13}$	10.5
842	95-026 13:47	3	2	19	8	11	8	9	9	7	0	1	0	0	1	0	1	0	1	2	5.08328	251.3	−0.1	1.06774	63	313	22	19.9	1.6	$6.3\cdot10^{-14}$	6.0
856	95-044 04:34	3	3	224	20	25	8	5	4	5	0	1	46	0	1	0	1	0	1	2	5.11381	252.1	−0.1	1.01536	135	307	−34	45.7	1.6	$9.2\cdot10^{-14}$	6.0
871	95-054 01:50	2	2	0	10	19	0	9	6	7	0	0	41	0	1	0	1	0	1	2	5.12990	252.6	−0.1	0.98569	999	999	999	12.7	1.9	$9.1\cdot10^{-13}$	10.5
875	95-061 06:24	2	2	20	13	21	0	9	5	6	0	0	41	0	1	0	1	0	1	2	5.14113	252.9	−0.1	0.96400	62	313	23	12.7	1.9	$2.2\cdot10^{-12}$	10.5
876	95-061 06:24	3	3	60	19	21	18	10	12	7	0	1	40	0	1	0	1	0	1	2	5.14113	252.9	−0.1	0.96400	6	269	55	3.8	1.6	$1.4\cdot10^{-10}$	6.0
878	95-061 19:21	2	3	40	21	12	11	7	15	0	1	1	59	31	1	0	1	0	1	2	5.14195	253.0	−0.1	0.96237	34	300	43	12.7	1.9	$1.8\cdot10^{-12}$	10.5
880	95-064 16:22	2	3	50	19	7	17	9	6	0	1	1	40	23	1	0	1	0	1	2	5.14632	253.1	−0.1	0.95366	20	287	50	7.2	1.9	$2.9\cdot10^{-12}$	10.5
882	95-066 15:50	3	2	242	13	20	1	8	6	7	0	1	38	0	1	0	1	0	1	2	5.14929	253.2	−0.1	0.94766	110	315	−15	19.0	1.9	$5.1\cdot10^{-13}$	10.5
884	95-068 06:39	2	2	164	10	15	0	8	9	7	0	0	38	0	1	0	1	0	1	2	5.15170	253.3	−0.1	0.94275	219	219	−38	24.4	1.6	$7.0\cdot10^{-14}$	6.0
886	95-069 12.51	3	3	252	20	24	10	6	5	6	0	1	45	0	1	0	1	0	1	2	5.15356	253.3	−0.1	0.93893	96	316	−4	32.6	1.6	$3.0\cdot10^{-13}$	6.0
887	95-071 07:59	2	2	204	8	11	0	9	9	7	0	0	0	0	1	0	1	0	1	2	5.15619	253.4	−0.1	0.93346	163	284	−51	19.9	1.6	$6.3\cdot10^{-14}$	6.0
889	95-073 16:04	3	2	10	12	20	1	9	5	7	0	1	40	0	1	0	1	0	1	2	5.15958	253.5	−0.1	0.92634	76	315	11	12.7	1.9	$1.5\cdot10^{-12}$	10.5
891	95-075 11:13	3	2	229	10	15	1	8	9	6	0	1	39	0	1	0	1	0	1	2	5.16215	253.6	0.0	0.92086	128	310	−29	24.4	1.6	$7.0\cdot10^{-14}$	6.0
892	95-076 08:47	3	2	184	9	14	1	8	9	7	0	1	36	0	1	0	1	0	1	2	5.16343	253.6	0.0	0.91812	191	246	−52	24.4	1.6	$5.4\cdot10^{-14}$	6.0
905	95-083 13:21	3	2	26	12	20	7	8	5	6	0	1	40	0	1	0	1	0	1	2	5.17344	254.0	0.0	0.89611	53	310	29	19.0	1.9	$4.3\cdot10^{-13}$	10.5
917	95-085 17:07	2	2	162	10	13	0	8	9	7	0	0	36	0	1	0	1	0	1	2	5.17637	254.1	0.0	0.88949	222	218	−36	24.4	1.6	$5.3\cdot10^{-14}$	6.0
957	95-088 18:27	2	2	223	13	8	11	10	10	0	1	1	43	22	1	0	1	0	1	2	5.18046	254.2	0.0	0.88009	136	306	−35	9.7	1.9	$7.3\cdot10^{-13}$	10.5
961	95-089 03:05	2	2	75	9	6	4	10	15	0	1	1	38	31	1	0	1	0	1	2	5.18094	254.2	0.0	0.87899	345	241	52	9.7	1.9	$2.7\cdot10^{-13}$	10.5
971	95-091 11:10	2	2	128	10	4	7	10	3	0	1	1	0	0	1	0	1	0	1	2	5.18401	254.4	0.0	0.87179	270	206	0	9.7	1.9	$2.3\cdot10^{-13}$	10.5
997	95-093 19:15	2	2	9	10	13	9	10	15	0	1	1	61	31	1	0	1	0	1	2	5.18704	254.5	0.0	0.86458	77	316	10	4.7	1.7	$9.0\cdot10^{-12}$	6.7
1023	95-099 21:56	2	2	105	9	0	9	9	0	0	0	1	0	0	1	0	1	0	1	2	5.19477	254.7	0.0	0.84567	302	211	26	12.7	1.9	$4.9\cdot10^{-13}$	10.5
1070	95-103 16:31	3	2	35	13	4	1	8	15	9	0	1	17	2	1	0	1	0	1	2	5.19940	254.9	0.0	0.83396	41	304	38	19.0	1.9	$5.6\cdot10^{-14}$	10.5
1079	95-107 02:30	2	2	73	12	12	13	12	15	0	1	1	12	31	1	0	1	0	1	2	5.20351	255.1	0.0	0.82334	347	244	53	4.5	1.9	$1.2\cdot10^{-11}$	10.5
1083	95-110 21:05	3	3	254	21	26	28	4	4	5	0	1	46	0	0	0	1	0	1	2	5.20794	255.3	0.0	0.81158	93	316	−1	52.6	1.6	$6.8\cdot10^{-14}$	6.0
1089	95-120 14:03	3	3	7	19	23	7	7	7	6	0	1	44	0	1	0	1	0	1	2	5.21884	255.7	0.0	0.78120	80	316	8	19.9	1.6	$1.4\cdot10^{-12}$	6.0
1092	95-122 09:11	3	3	86	20	24	4	6	4	6	0	1	45	0	1	0	1	0	1	2	5.22078	255.8	0.0	0.77556	329	225	45	36.5	1.6	$2.0\cdot10^{-13}$	6.0
1121	95-140 12:55	3	2	19	13	21	2	8	4	5	0	1	41	0	1	0	1	0	1	2	5.23904	256.6	0.0	0.71820	63	313	22	19.0	1.9	$6.1\cdot10^{-13}$	10.5
1122	95-142 21:00	3	2	200	11	15	3	8	9	7	0	1	38	0	1	0	1	0	1	2	5.24122	256.7	0.0	0.71077	169	277	−53	24.4	1.6	$8.2\cdot10^{-14}$	6.0
1130	95-148 10:44	2	2	247	8	6	1	10	15	0	1	1	43	31	1	0	1	0	1	2	5.24623	257.0	0.0	0.69302	103	316	−9	9.7	1.9	$2.3\cdot10^{-13}$	10.5
1207	95-181 21:09	2	2	193	9	11	8	10	10	1	1	1	0	0	1	0	1	0	1	2	5.27147	258.5	0.1	0.58526	179	254	−54	16.0	1.6	$1.7\cdot10^{-13}$	6.0
1217	95-198 22:59	2	2	0	9	9	1	7	9	3	1	1	6	31	1	0	1	0	1	2	5.28116	259.2	0.1	0.52938	999	999	999	29.8	1.9	$1.2\cdot10^{-14}$	10.5
1452	95-219 19:25	2	2	162	8	10	4	8	9	4	1	1	0	0	1	0	1	0	1	2	5.28967	260.2	0.1	0.46020	222	208	−36	24.4	1.6	$2.4\cdot10^{-14}$	6.0
1453	95-219 23:44	2	2	239	12	21	10	11	15	0	1	1	45	31	1	0	1	0	1	2	5.28972	260.2	0.1	0.45960	114	305	−18	7.2	1.9	$8.1\cdot10^{-12}$	10.5
1459	95-220 08:21	2	2	85	8	9	12	7	9	3	1	1	6	31	1	0	1	0	1	2	5.28983	260.2	0.1	0.45839	330	217	45	29.8	1.9	$1.0\cdot10^{-14}$	10.5

continued over

Table 5
Continued

No.	IMP. DATE	CLN	AR	SEC	IA	EA	CA	IT	ET	EIT	EIC	ICC	PA	PET	EVD	ICP	ECP	CCP	PCP	HV	R	LON	LAT	D_{Jup}	ROT	S_{LON}	S_{LAT}	V	VEF	M	MEF
1585	95-225 17:47	2	2	70	8	0	13	7	0	0	0	1	5	31	1	0	1	0	1	2	5.29140	260.4	0.1	0.44031	352	240	54	29.8	1.9	$1.8\cdot10^{-14}$	10.5
1633	95-226 23:59	2	2	119	12	11	1	10	15	0	1	1	45	31	1	0	1	0	1	2	5.29174	260.5	0.1	0.43608	283	198	10	9.7	1.9	$1.0\cdot10^{-12}$	10.5
1707	95-229 21:00	2	2	0	14	21	10	8	4	6	0	1	40	0	1	0	1	0	1	2	5.29246	260.6	0.2	0.42641	999	999	999	19.0	1.9	$7.2\cdot10^{-13}$	10.5
1758	95-231 16:09	2	2	24	11	14	2	13	15	0	1	1	58	31	1	0	1	0	1	2	5.29287	260.7	0.2	0.42035	56	302	27	2.3	1.6	$1.5\cdot10^{-10}$	6.0
1887	95-237 23:08	2	2	104	8	12	0	9	9	6	0	0	36	0	1	0	1	0	1	2	5.29415	260.9	0.2	0.39908	304	202	27	19.9	1.6	$7.4\cdot10^{-14}$	6.0
1888	95-238 12:05	2	2	75	8	11	0	8	9	5	0	0	7	31	1	0	1	0	1	2	5.29424	261.0	0.2	0.39725	345	231	52	24.4	1.6	$2.8\cdot10^{-14}$	6.0
1889	95-238 16:24	2	2	82	8	9	4	8	9	3	1	1	0	0	1	0	1	0	1	2	5.29428	261.0	0.2	0.39664	335	221	48	19.0	1.9	$5.6\cdot10^{-14}$	10.5
1919	95-240 02:54	2	2	30	9	13	0	9	9	7	0	0	36	0	1	0	1	0	1	2	5.29452	261.0	0.2	0.39176	48	299	33	19.9	1.6	$1.0\cdot10^{-13}$	6.0
1948	95-241 04:47	2	2	121	8	13	0	8	8	7	0	0	37	0	1	0	1	0	1	2	5.29469	261.1	0.2	0.38810	280	198	8	26.4	1.6	$2.9\cdot10^{-14}$	6.0
1997	95-247 20:25	3	2	154	8	13	1	8	8	6	0	1	36	0	1	0	1	0	1	2	5.29555	261.4	0.2	0.36545	233	203	−28	26.4	1.6	$2.9\cdot10^{-14}$	6.0
1998	95-250 04:30	2	2	126	8	13	0	8	8	6	0	0	36	0	1	0	1	0	1	2	5.29577	261.5	0.2	0.35746	273	197	2	26.4	1.6	$2.9\cdot10^{-14}$	6.0
2067	95-253 18:46	2	2	7	8	10	5	10	11	0	1	1	4	31	1	0	1	0	1	2	5.29603	261.6	0.2	0.34514	80	307	8	14.0	1.6	$1.9\cdot10^{-13}$	6.0
2203	95-270 16:18	2	2	15	10	12	5	9	10	0	1	1	0	0	1	0	1	0	1	2	5.29595	262.3	0.2	0.28667	69	305	17	18.3	1.6	$1.5\cdot10^{-13}$	6.0
2359	95-281 11:08	2	2	210	8	4	0	6	14	12	0	0	0	0	1	0	1	0	1	2	5.29475	262.8	0.2	0.24878	155	284	−47	39.6	1.9	$1.6\cdot10^{-15}$	10.5
2382	95-291 04:06	3	2	251	14	22	7	9	4	7	0	1	42	0	1	0	1	0	1	2	5.29291	263.2	0.2	0.21417	97	317	−6	12.7	1.9	$3.0\cdot10^{-12}$	10.5
2384	95-291 12:44	3	2	107	8	12	1	8	8	6	0	1	0	0	1	0	1	0	1	2	5.29282	263.2	0.2	0.21288	300	212	23	26.4	1.6	$2.5\cdot10^{-14}$	6.0
2429	95-304 19:58	2	2	53	9	10	4	10	11	0	1	1	0	0	1	0	1	0	1	2	5.28905	263.8	0.3	0.16438	15	284	51	9.7	1.9	$5.3\cdot10^{-13}$	10.5
2457	95-310 01:05	1	2	64	9	5	0	10	12	0	1	0	12	22	1	0	1	0	1	2	5.28718	264.0	0.3	0.14490	0	264	53	9.7	1.9	$2.3\cdot10^{-13}$	10.5
2484	95-312 22:06	3	2	156	10	19	7	9	7	6	0	1	38	0	1	0	1	0	1	2	5.28606	264.1	0.3	0.13401	231	215	−31	12.7	1.9	$9.1\cdot10^{-13}$	10.5
2497	95-315 10:30	2	2	86	11	5	10	10	15	0	1	1	39	30	1	0	1	0	1	2	5.28502	264.2	0.3	0.12437	329	228	43	9.7	1.9	$3.1\cdot10^{-13}$	10.5
2509	95-318 03:13	2	2	192	14	5	5	8	15	0	1	1	42	30	1	0	1	0	1	2	5.28385	264.3	0.3	0.11392	180	264	−56	19.0	1.9	$7.6\cdot10^{-14}$	10.5
2599	95-330 04:15	3	4	189	30	54	17	9	5	5	0	1	47	0	1	0	1	0	1	2	5.27793	264.7	0.3	0.06475	184	257	−55	7.2	1.9	$1.6\cdot10^{-09}$	10.5
2600	95-331 19:05	2	2	90	9	5	4	9	15	0	1	1	5	31	1	0	1	0	1	2	5.27706	264.8	0.3	0.05764	323	224	40	12.7	1.9	$1.2\cdot10^{-13}$	10.5
2676	95-337 08:49	1	2	165	8	5	0	7	11	0	1	0	0	0	1	0	1	0	1	2	5.27410	264.9	0.3	0.03106	218	221	−40	29.8	1.9	$5.1\cdot10^{-15}$	10.5
2704	95-338 23:39	2	2	71	8	0	14	8	0	0	0	1	0	0	1	0	1	0	1	2	5.27339	265.0	0.3	0.02218	350	250	52	19.0	1.9	$1.0\cdot10^{-13}$	10.5
2756	95-341 03:17	3	2	20	9	4	12	6	6	10	0	1	6	31	5	2	2	0	2	1	5.27337	265.0	0.3	0.00798	62	315	22	39.6	1.9	$1.9\cdot10^{-15}$	10.5
2759	95-341 03:24	3	2	99	8	12	1	6	8	8	0	1	8	31	5	2	2	0	2	1	5.27338	265.0	0.3	0.00795	311	217	31	38.1	1.6	$6.8\cdot10^{-15}$	6.0
2760	95-341 07:43	3	3	111	22	25	20	6	7	8	0	1	46	0	5	2	2	0	2	1	5.27361	265.0	0.3	0.00647	294	212	18	24.4	1.6	$1.3\cdot10^{-12}$	6.0
2761	95-341 12:01	3	2	120	12	19	12	7	8	10	0	1	38	0	5	2	2	0	2	1	5.27399	265.0	0.3	0.00493	281	209	8	29.8	1.9	$6.4\cdot10^{-14}$	10.5
2763	95-341 15:15	1	2	73	8	12	1	14	12	0	1	0	17	31	5	2	2	0	2	1	5.27448	265.0	0.3	0.00372	347	247	52	4.9	2.1	$5.0\cdot10^{-12}$	14.3
2765	95-341 15:17	1	2	122	9	11	1	14	15	0	1	0	19	31	5	2	2	0	2	1	5.27449	265.0	0.3	0.00371	278	209	6	2.1	1.6	$9.1\cdot10^{-11}$	6.0
2767	95-341 15:19	1	2	134	11	12	1	14	15	0	1	0	9	31	5	2	2	0	2	1	5.27449	265.0	0.3	0.00370	262	209	−7	2.0	1.9	$2.0\cdot10^{-10}$	10.5
2768	95-341 15:22	1	2	60	11	13	1	14	15	0	1	0	18	31	5	2	2	0	2	1	5.27450	265.0	0.3	0.00368	6	271	53	2.1	1.6	$1.7\cdot10^{-10}$	6.0
2769	95-341 15:25	1	2	168	13	15	1	15	15	0	1	0	6	31	5	2	2	0	2	1	5.27451	265.0	0.3	0.00366	214	224	−43	2.1	1.6	$3.2\cdot10^{-10}$	6.0
2772	95-341 15:29	1	2	214	11	14	1	14	15	0	1	0	17	31	5	2	2	0	2	1	5.27453	265.0	0.3	0.00364	149	301	−45	2.1	1.6	$2.0\cdot10^{-10}$	6.0
2775	95-341 15:30	1	2	104	13	21	1	15	14	0	1	0	11	31	5	2	2	0	2	1	5.27453	265.0	0.3	0.00363	304	214	26	2.0	1.9	$8.1\cdot10^{-10}$	10.5
2777	95-341 15:32	1	2	166	14	21	1	15	15	0	1	0	41	31	5	2	2	0	2	1	5.27454	265.0	0.3	0.00362	217	222	−41	2.0	1.9	$9.5\cdot10^{-10}$	10.5
2780	95-341 15:54	3	4	110	25	29	22	8	8	9	0	1	47	0	5	2	2	0	2	1	5.27461	265.0	0.3	0.00348	295	212	20	16.0	1.6	$2.1\cdot10^{-11}$	6.0
2782	95-341 16:08	2	2	116	9	23	1	7	0	8	0	0	11	0	5	2	2	0	2	1	5.27466	265.0	0.3	0.00340	287	210	13	29.8	1.9	$7.9\cdot10^{-14}$	10.5
2786	95-341 16:45	2	2	91	13	19	1	15	15	14	0	0	17	2	5	2	2	0	2	1	5.27481	265.0	0.3	0.00317	322	223	39	2.5	1.6	$2.1\cdot10^{-10}$	6.0
2791	95-341 17:21	2	2	194	8	22	1	7	3	9	0	0	12	0	5	2	2	0	2	1	5.27497	265.0	0.3	0.00296	177	268	−55	29.8	1.9	$5.6\cdot10^{-14}$	10.5
2793	95-341 17:25	1	2	64	8	22	1	6	12	15	0	0	8	0	5	2	2	0	2	1	5.27499	265.0	0.3	0.00293	0	264	53	39.6	1.9	$2.0\cdot10^{-14}$	10.5
2795	95-341 17:28	1	2	193	10	7	1	6	13	15	0	0	10	0	5	2	2	0	2	1	5.27501	265.0	0.3	0.00291	179	266	−56	39.6	1.9	$3.6\cdot10^{-15}$	10.5
2799	95-341 17:40	1	2	12	11	26	1	7	15	7	0	1	13	0	5	2	2	0	2	1	5.27507	265.0	0.3	0.00285	73	317	13	29.8	1.9	$1.8\cdot10^{-13}$	10.5
2803	95-341 17:42	2	2	157	9	7	1	10	10	12	0	0	41	0	5	2	2	0	2	1	5.27508	265.0	0.3	0.00283	229	216	−32	9.7	1.9	$3.3\cdot10^{-13}$	10.5
2805	95-341 17:43	2	2	15	8	22	1	6	3	9	0	1	10	0	5	2	2	0	2	1	5.27508	265.0	0.3	0.00283	69	316	16	39.6	1.9	$2.0\cdot10^{-14}$	10.5
2806	95-341 17:44	2	2	151	10	9	1	9	8	0	1	1	41	24	5	2	2	0	2	1	5.27509	265.0	0.3	0.00282	238	213	−26	12.7	1.9	$2.8\cdot10^{-13}$	10.5
2808	95-341 17:44	1	3	46	19	22	1	4	12	12	0	1	21	0	5	2	2	0	2	1	5.27509	265.0	0.3	0.00282	25	294	46	11.3	3.7	$6.7\cdot10^{-12}$	105.1
2809	95-341 17:45	2	2	147	9	11	1	7	15	8	0	1	8	31	5	2	2	0	2	1	5.27509	265.0	0.3	0.00282	243	211	−22	8.3	3.9	$9.4\cdot10^{-13}$	120.2
2811	95-341 17:45	1	3	220	19	28	1	6	14	15	0	0	7	31	5	2	2	0	2	1	5.27509	265.0	0.3	0.00282	141	307	−39	19.0	1.9	$3.9\cdot10^{-12}$	10.5
2817	95-341 17:46	2	4	119	26	1	1	15	0	0	1	1	12	5	5	2	2	0	2	1	5.27510	265.0	0.3	0.00281	283	210	9	2.0	1.9	$2.7\cdot10^{-10}$	10.5

2818	95-341 17:46	1	3	118	19	30	1	5	1	6	1	0	21	0	5	2	2	0	2	1	5.27510	265.0	0.3	0.00281	284	210	11	29.8	1.9	$9.1\cdot10^{-13}$	10.5
2820	95-341 17:46	1	2	223	8	20	1	6	4	11	0	1	9	0	5	2	2	0	2	1	5.27510	265.0	0.3	0.00281	136	309	−37	39.6	1.9	$1.4\cdot10^{-14}$	10.5
2821	95-341 17:47	1	4	57	26	1	1	15	0	0	1	0	6	30	5	2	2	0	2	1	5.27510	265.0	0.3	0.00280	10	277	52	2.0	1.9	$2.7\cdot10^{-10}$	10.5
2823	95-341 17:47	1	2	208	9	6	1	7	4	15	0	0	12	0	5	2	2	0	2	1	5.27510	265.0	0.3	0.00280	158	293	−50	29.8	1.9	$7.3\cdot10^{-15}$	10.5
2824	95-341 17:50	1	3	176	20	1	1	3	15	15	1	0	21	30	5	2	2	0	2	1	5.27512	265.0	0.3	0.00279	203	234	−50	70.0	1.9	$4.8\cdot10^{-16}$	10.5
2825	95-341 17:50	2	2	52	9	12	5	9	14	12	0	1	5	31	5	2	2	0	2	1	5.27512	265.0	0.3	0.00279	17	285	50	6.4	1.6	$2.5\cdot10^{-12}$	6.0
2826	95-341 17:54	1	2	40	12	27	1	7	15	6	0	0	14	0	5	2	2	0	2	1	5.27514	265.0	0.3	0.00276	34	301	42	29.8	1.9	$2.5\cdot10^{-13}$	10.5
2827	95-341 17:55	2	2	92	11	7	1	8	14	12	0	1	5	31	5	2	2	0	2	1	5.27514	265.0	0.3	0.00276	321	222	38	19.0	1.9	$6.7\cdot10^{-14}$	10.5
2829	95-341 17:57	1	2	61	8	21	1	13	3	15	0	0	10	0	5	2	2	0	2	1	5.27516	265.0	0.3	0.00275	4	269	53	2.3	1.9	$1.9\cdot10^{-10}$	10.5
2830	95-341 17:58	3	3	74	19	21	11	6	7	9	0	1	41	0	5	2	2	0	2	1	5.27516	265.0	0.3	0.00274	346	245	51	24.4	1.6	$4.3\cdot10^{-13}$	6.0
2835	95-341 18:06	1	2	171	15	21	1	12	15	0	1	0	47	31	5	2	2	0	2	1	5.27521	265.0	0.3	0.00270	210	228	−46	3.8	1.6	$9.5\cdot10^{-11}$	6.0
2838	95-341 20:34	2	2	164	10	5	1	7	5	14	0	0	4	30	5	2	2	0	2	1	5.27626	265.0	0.3	0.00203	219	221	−39	29.8	1.9	$7.1\cdot10^{-15}$	10.5
2840	95-341 20:39	3	3	73	19	20	1	8	12	10	0	1	39	0	5	2	2	0	2	1	5.27631	265.0	0.3	0.00202	347	247	52	9.7	1.9	$6.8\cdot10^{-12}$	10.5
2841	95-341 20:39	1	2	34	8	0	1	7	0	0	0	0	6	29	5	2	2	0	2	1	5.27631	265.0	0.3	0.00202	42	307	36	29.8	1.9	$1.8\cdot10^{-14}$	10.5
2842	95-341 20:39	3	5	154	54	59	27	13	5	5	0	1	47	0	5	2	2	0	2	1	5.27631	265.0	0.3	0.00202	233	214	−29	10.6	7.7	$6.8\cdot10^{-09}$	1303.9
2844	95-341 20:40	2	2	78	8	9	1	7	13	11	0	0	4	28	5	2	2	0	2	1	5.27632	265.0	0.3	0.00201	340	239	49	29.8	1.9	$1.0\cdot10^{-14}$	10.5
2845	95-341 20:40	1	2	88	8	0	1	7	0	0	0	0	7	29	5	2	2	0	2	1	5.27632	265.0	0.3	0.00201	326	226	42	29.8	1.9	$1.8\cdot10^{-14}$	10.5
2846	95-341 20:40	3	3	95	19	20	13	8	12	10	0	1	38	0	5	2	2	0	2	1	5.27632	265.0	0.3	0.00201	316	220	35	9.7	1.9	$6.8\cdot10^{-12}$	10.5
2847	95-341 20:41	2	2	179	8	6	1	7	13	10	0	0	8	28	5	2	2	0	2	1	5.27633	265.0	0.3	0.00201	198	239	−51	29.8	1.9	$6.2\cdot10^{-15}$	10.5
2854	95-341 23:27	2	2	37	8	6	1	7	14	10	0	0	6	29	5	2	2	0	2	X	5.27810	265.0	0.3	0.00207	38	304	39	29.8	1.9	$6.2\cdot10^{-15}$	10.5
2857	95-341 23:30	2	2	249	8	6	1	7	14	10	0	0	9	28	5	2	2	0	2	X	5.27814	265.0	0.3	0.00208	100	318	−8	29.8	1.9	$6.2\cdot10^{-15}$	10.5
2859	95-341 23:32	1	2	196	14	12	0	15	9	0	1	0	42	30	5	2	2	0	2	X	5.27816	265.0	0.3	0.00209	174	272	−55	2.0	1.9	$3.3\cdot10^{-10}$	10.5
2861	95-341 23:35	2	6	222	58	60	1	5	5	4	1	1	1	0	5	2	2	0	2	X	5.27819	265.0	0.3	0.00210	138	308	−37	40.9	1.6	$1.9\cdot10^{-10}$	6.0
2868	95-342 00:11	2	5	0	49	59	0	7	4	5	0	0	49	0	5	2	2	0	2	X	5.27859	265.0	0.3	0.00224	999	999	999	11.8	11.8	$2.2\cdot10^{-09}$	5858.3
2876	95-342 13:56	2	2	0	9	9	1	10	12	11	0	0	17	25	5	2	2	0	2	X	5.28441	265.0	0.3	0.00681	999	999	999	9.7	1.9	$4.5\cdot10^{-13}$	10.5
2877	95-342 13:56	1	2	0	9	13	1	14	15	0	1	0	17	30	5	2	2	0	2	X	5.28441	265.0	0.3	0.00681	999	999	999	2.1	1.6	$1.3\cdot10^{-10}$	6.0
2878	95-342 18:14	2	2	0	12	7	0	14	15	10	0	0	5	29	5	2	2	0	2	X	5.28559	265.1	0.3	0.00811	999	999	999	2.0	1.9	$1.1\cdot10^{-10}$	10.5
2879	95-343 07:11	1	2	60	14	15	1	15	15	0	1	0	41	31	5	2	2	0	2	X	5.28842	265.1	0.3	0.01162	6	271	53	2.0	1.9	$5.1\cdot10^{-10}$	10.5
2880	95-343 07:11	2	2	253	10	24	0	7	4	9	0	0	46	0	5	2	2	0	2	X	5.28842	265.1	0.3	0.01162	94	319	−3	29.8	1.9	$1.1\cdot10^{-13}$	10.5
2882	95-346 21:28	2	2	219	8	6	0	7	15	11	0	0	0	0	5	2	2	0	2	X	5.29890	265.6	0.3	0.02828	142	306	−40	29.8	1.9	$6.2\cdot10^{-15}$	10.5

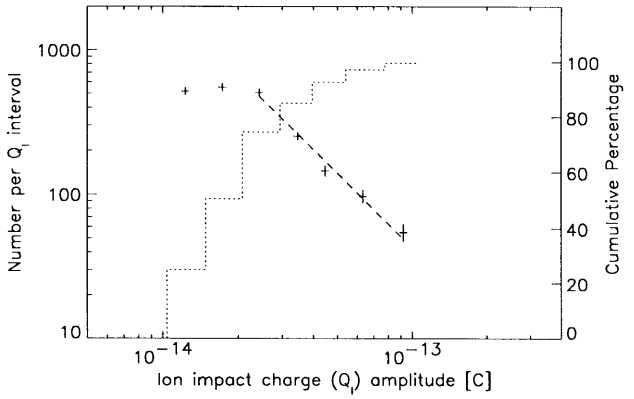

Fig. 6. Same as Fig. 5 but for the small particles in the lowest amplitude range (AR1) only. A power law fit to the data with 2×10^{-14} C $< Q_I < 10^{-13}$ C is shown as a dashed line (power law index -1.9).

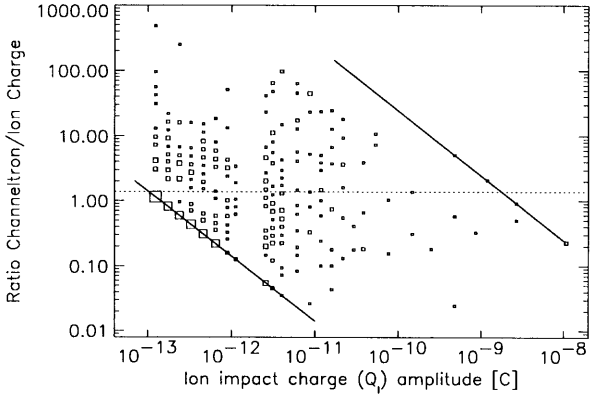

Fig. 7. Channeltron amplification factor $A = Q_C/Q_I$ as a function of impact charge Q_I for big particles (AR2–AR6) detected between 1993–95. The solid lines indicate the sensitivity threshold (lower left) and the saturation limit (upper right) of the channeltron. Squares indicate dust particle impacts and the area of the squares is proportional to the number of events (the scaling of the squares is not the same as in Paper II). The dotted horizontal line shows the mean value of the channeltron amplification $A = 1.4$ for ion impact charges 10^{-12} C $< Q_I < 10^{-10}$ C.

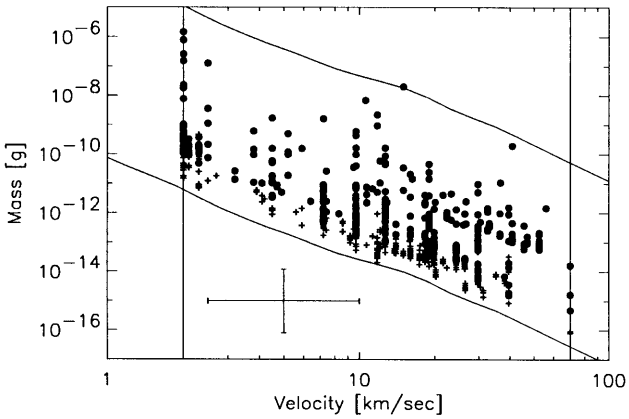

Fig. 8. Masses and impact speeds of all impacts recorded by DDS between 1993–95. The lower and upper solid lines indicate the threshold and saturation limits of the detector, respectively, and the vertical lines indicate the calibrated velocity range. A sample error bar is shown that indicates a factor of 2 error for the velocity and a factor of 10 for the mass determination. Note that the small particles (plus signs) are probably faster and smaller than implied by this diagram (see text for details).

neglect the large number of small particles in the lowest amplitude range in Fig. 7 because they do not contribute to the determination of the channeltron amplification. Their neglect better illustrates the number distribution of impacts in the higher amplitude ranges.

Figure 8 displays the masses and velocities of all dust particles detected between 1993–95. As in the earlier period (1990–92), velocities occur over the entire calibrated range from 2–70 km/s and the masses vary over 10 orders of magnitude from 10^{-6}–10^{-16} g. The mean errors are a factor of 2 for the velocity and a factor of 10 for the mass. The clustering of the velocity values is due to discrete steps in the rise time measurement but this quantization is much smaller than the velocity uncertainty. Masses and velocities in the lowest amplitude range (particles indicated by plus signs) should be treated with caution. These are mostly Jovian stream particles for which we have clear indications that their masses and velocities are outside the calibrated range of DDS (Zook et al., 1996). The particles are probably much faster and smaller than implied by Fig. 8. On the other hand, the mass velocity calibration is valid for the bigger particles. For many particles in the lowest two amplitude ranges (AR1 and AR2) the velocity had to be computed from the ion charge signal alone which leads to the striping in the lower mass range in Fig. 8 (most prominent above 10 km/s). In the higher amplitude ranges the velocity could normally be calculated from both the target and the ion charge signal which leads to a more continuous distribution in the mass-velocity plane. Impact velocities below about 3 km/s should be treated with caution because anomalous impacts onto the sensor grids or structures other than the target generally lead to prolonged rise times and hence to artificially low impact velocities.

The sensor orientation (rotation angle) at the time of particle impact is shown in Fig. 9. Particles approaching parallel to the ecliptic plane are detected at rotation angles of 90 and 270°. Contour lines illustrate the detector sensitivity for interstellar particles. The impact direction of most of the big particles (filled circles) is compatible with the interstellar direction. The remaining big particles are compatible with an interplanetary origin. Baguhl et al. (1996) showed that in the outer solar system (i.e., outside about 2.6 AU from the Sun), interstellar particles can be clearly distinguished from particles having interplanetary origin. At distances between 1 and 2.6 AU, however, interplanetary dust particles on prograde orbits approach from the same direction as interstellar particles and both populations cannot be separated by impact direction arguments. In contrast to the small stream par-

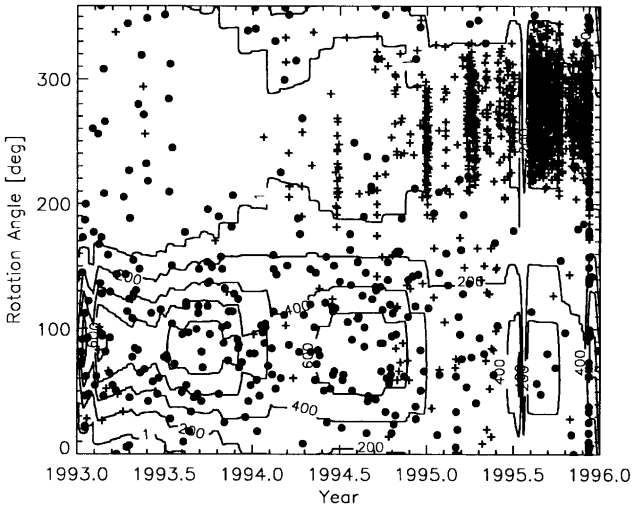

Fig. 9. Rotation angles vs time for two different mass ranges (filled circles: big particles, AR2 to AR6; plus signs: small particles, AR1). See Section 2 for an explanation of the rotation angle. The dust streams show up as vertical bands with plus signs. For some time periods, no rotation angle information was available; these data are not shown. The contour lines show the sensitive area of DDS for interstellar particles (levels of 1, 200, 400, 600 and 800 cm^2 detector area are shown). The number of big impacts is depressed during the dust streams because of deadtime caused by the large number of small impacts.

ticles which are outside the calibrated range of DDS, the calibration is valid for the interplanetary and interstellar particles (cf. Table 5).

The small particles (plus signs) cluster at rotation angles between 200–340° which is compatible with a Jovian origin (Grün et al., 1996a). The striping of small impacts (plus signs) is due to the occurrence of individual dust streams, and a comparison with Fig. 4 shows that the times of the stripes are coincident with the times of high impact rates. At the end of 1995, the impact rates were so high over several weeks that the symbols form a black area in Fig. 9.

5. Io and Jupiter flybys

On 7 December 1995, Galileo arrived at Jupiter after its six-year journey through interplanetary space. Because of the expected increase in the high energy electron flux near Jupiter the channeltron high voltage of DDS was reduced and the detection thresholds were increased on 6 December, 5:40 h (Table 2). At that time, Galileo was at a distance of 15 R_J from Jupiter (Jupiter radius, $R_J = 71{,}492$ km). The change in the instrument configuration led to a reduction in sensitivity by about a factor of six. On 7 December, 17:46 h, Galileo flew by Io and at 21:54 h nearest to Jupiter. At 23:25 h the channeltron high voltage was switched off and at 00:27 h on 8 December, the orbit insertion maneuver was started which brought Galileo into a bound orbit about Jupiter.

From 1–6 December 1995, MROs occurred about once per day. Around the time of Galileo's closest approach to Io on 7 December DDS data were read out every few minutes and recorded to Galileo's tape recorder (record period, 15:21–18:25 h). After Jupiter closest approach (21:54 h), data were recorded for another two h (23:22–01:26 h). The recorded data from both flybys were transmitted to Earth a few months later. Initial results from the Io and Jupiter flybys have been published by Grün et al. (1996b).

Figure 10 shows the dust impact rate before and around the Io and Jupiter flybys. During Galileo's approach to Jupiter, the impact rate increased considerably and reached a maximum of about 200 impacts per day on 4 December 1995 (day 338). Two days later the sensitivity of the instrument was reduced and the impact rate dropped by about a factor of 10. After the sensitivity reduction a few small particle were still being detected until closest approach to Io. At Io closest approach, small particle impacts ceased. Big particles were only detected a few days before closest approach to Io when Galileo was within about 25 R_J of Jupiter. The big particles show a concentration towards the inner Jovian system. Impacts of big particles were seen after Io flyby until closest approach to Jupiter, i.e., when impacts of small class 3 particles had already terminated. High impact rates of small particles and increases in the impact rate upon approach towards the inner Jovian System were also seen later during Galileo's orbital tour about the planet (Grün et al., 1997; 1998). Concentrations of big particles between the Galilean satellites have also been found. For the calculation of the impact rate in Fig. 10 we have only considered the class 3 impacts because

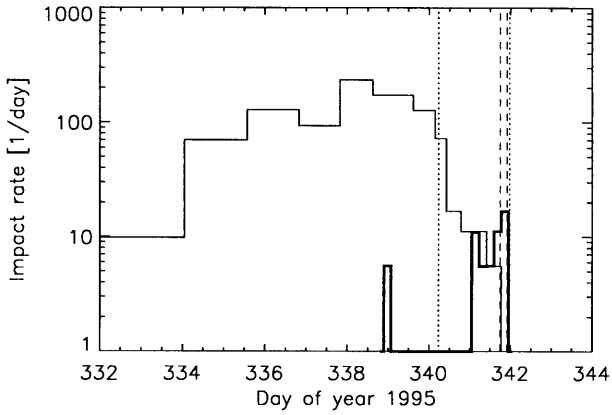

Fig. 10. Dust impact rate vs time for a period of 12 days around Galileo's approach towards the inner Jovian system as obtained from the impact accumulators. The thin solid lines show the impact rate of small particles (AR1) and the heavy solid lines shows that of big particles (AR2 to AR6). Because high noise rates in classes 1 and 2 occurred on days 340–342, only class 3 impacts are shown here. The times of closest approaches to Io and Jupiter are indicated by dashed lines, and times when the detector sensitivity was reduced are shown as dotted lines. Note that the peak in the impact rate of big particles on day 339.0 is produced by only one impact.

classes 1 and 2 show evidence for contamination by noise in the inner Jovian system (see below). The inclusion of big class 2 events—which seem to be less affected by noise—would increase the number of impacts per given time interval (cf. Table 3) but would not change our conclusions about the cessation of small dust impacts after Io and Jupiter flybys (Grün et al., 1996b).

In Fig. 11, we show the rotation angle of the class 3 impacts for which the complete information has been transmitted to Earth. When Galileo was approaching Jupiter, the impact directions of dust particles were concentrated between 210–350°. About one day before closest approach to Io, two particles also arrived from the opposite direction. The striping before day 341 is due to the occurrence of MROs once per day—which allow for a time resolution of 4.3 h—and the fact that the instrument memory of DDS can store only 16 class 3 events. Note that each vertical band of particles between days 332–340 in Fig. 11 corresponds to one discrete MRO. If there are more than 16 impacts between two MROs, the oldest events are lost. Before day 341, 15:20 h many class 3 particles have probably been lost. Note that the particle on day 339.0 that caused the peak in the impact rate of big particles in Fig. 10 cannot be shown because its full information has not been transmitted to Earth.

So far we have only considered class 3 impacts around Io and Jupiter flybys. During closest approach to Jupiter in December 1995 and during all later orbits, high noise rates occurred when Galileo was within about 20 R_J of Jupiter (cf. Grün et al., 1997). In Fig. 12 we show the rotation angle for all impact events in classes 1–3 for

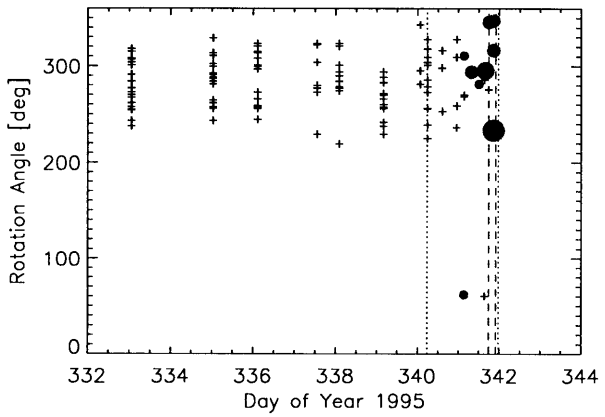

Fig. 11. Rotation angle vs time for 12 days around Galileo's approach towards the inner Jovian system. Only class 3 impacts are shown for which the full information has been transmitted to Earth. Plus signs indicate small particles (AR1) and filled circles show big particles (the symbol size denotes the amplitude range of the particle, AR2 and AR5). The times of closest approaches to Io and Jupiter are indicated by dashed lines, whereas times when the detector sensitivity was reduced are shown as dotted lines. The striping before day 341, 15:20 h is due to the occurrence of MROs once per day which allow for only 4.3 h time resolution and the fact that the instrument memory of DDS can store only 16 class 3 events. Many particles have probably been lost before day 341.

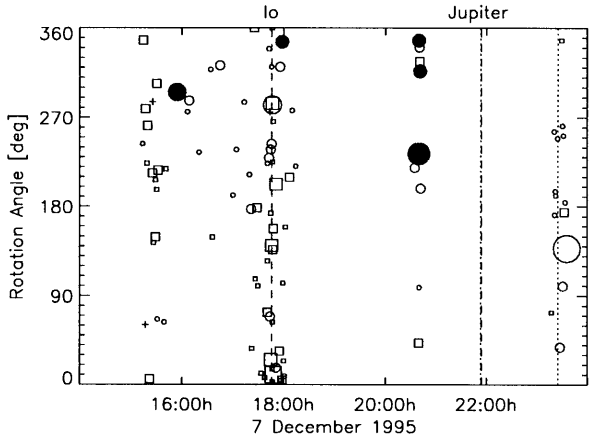

Fig. 12. Rotation angle vs time for a period of 12 h around Io closest approach on 7 Dec 1995 (day 341). The symbols have the following meaning: '+': class 3, AR1; '●': class 3, AR2 to AR5; '○': class 2; '□': class 1; the size of the symbols indicates the amplitude ranges of the particles, with AR1 being the smallest and AR6 being the biggest amplitude range occurring in the diagram. The times of closest approaches to Io and Jupiter are indicated by dashed lines and the time when the detector sensitivity was reduced is shown as a dotted line. Events at 20:40 h occurred in a gap when no data have been transmitted to Earth and their impact times have 4.3 h uncertainty. For the other particles the uncertainty in impact time is usually a few minutes, except for impacts at 15:20 and 23:20 h which have 70 and 33 min uncertainty, respectively (see text for details).

which the complete information is available for a period of half a day around closest approach to Io. The striping at 15:20 and 20:40 h is again due to discrete instrument readouts and the time resolution is usually 4.3 h. Because of the switch to record mode which occurred twice on day 341, the impact time can be determined with a higher accuracy from the internal timer of DDS: particles with impact times between 15:10–15:20 h must have impacted the detector between 14:11–15:21 h. Their uncertainty in impact time is only 70 min. Particles with impact times in the time interval 18:30–22:49 h have the full 4.3 h uncertainty, and those with impact times between 23:10–23:22 h must have been detected between 22:49–23:22 h; thus their timing uncertainty is only 33 min.

The class 1 impact events detected about 3 h before and at Io closest approach itself are spread over the whole range in rotation angles. At the same time the noise counter for the electron channel, which counts all threshold exceedings on that channel, detected a high noise rate in excess of 300 noise events per second. Furthermore, the class 1 event rate is strongly peaked at Io closest approach (Fig. 13). The event rate at Jupiter closest approach cannot be shown because no high resolution recorded data were obtained for that period.

The spread in rotation angle, the increased noise in the electron channel and the peak in impact rate indicate that at least some, if not all, of these events are due to noise rather than dust particle impacts. Although DDS can detect dust particles approaching from within 10° of Gal-

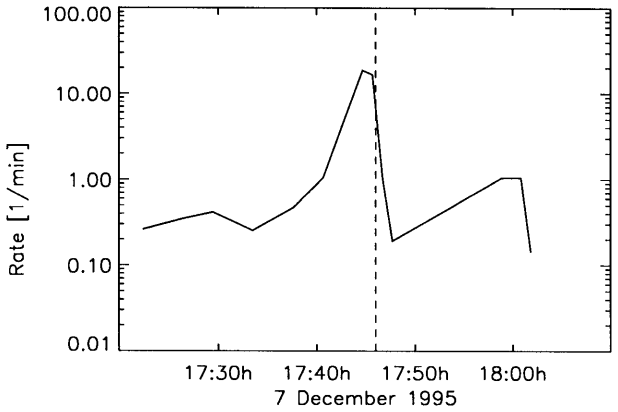

Fig. 13. Event rate of class 1 events for a period of 50 min around Io closest approach. The time of closest approach to Io is indicated by a dashed line.

ileo's positive spin axis at all rotation angles resulting in a 360° spread in a rotation angle plot, one can hardly imagine a population of dust particles that caused only class 1 events and none in class 3. If the class 1 events are due to real dust particles approaching from close to the positive spin direction, one should also see a similar spread in rotation angle for the class 3 particles, which is not the case. The smallest class 2 events (AR1) seem to follow a similar behavior as the class 1 events although much less obvious. Class 2 events also peak at Io closest approach but less strongly which is consistent with class 2 being less contaminated by noise than Class 1.

Similar signatures of noise contamination within about 20 R_J from Jupiter are evident in the DDS data from Galileo's later orbital tour in the Jovian system (cf. Grün et al., 1997). Therefore, all class 1 and 2 events detected in the Jovian system should be treated with caution. This applies to 26 class 1 and 20 class 2 events in Table 5 which were detected on days 341–343, and to 50 events in each class if one includes AR1 events and which are published only electronically. Only class 3 events can be considered good dust impacts at the moment. A detailed analysis of the noise characteristics of the DDS data from within the Jovian system is forthcoming.

6. Summary

In this paper, which is the fourth is a series of Galileo and Ulysses papers, we present data from the Galileo dust instrument for the period January 1993–December 1995 when Galileo was traversing interplanetary space between Earth and Jupiter. The complete information (i.e., all impact parameters measured by the dust instrument) for 395 big particles detected during this period is given (including 47 class 1 and 2 events around Io and Jupiter flybys which are possibly noise events). The full data set that contains 2525 small and big particles is available in electronic form only. Together with the 358 particles published in Paper II a set of 2883 particles detected during Galileo's six years' journey to Jupiter is now available. Our results can be summarized as follows:

(1) A relatively constant impact rate of interplanetary and interstellar particles of 0.4 impacts per day was detected over the whole three-year time span. In the outer solar system (outside about 2.6 AU) the big particles are mostly of interstellar origin, whereas in the inner solar system interplanetary particles dominate. These particles are in the calibrated mass and velocity range of DDS.
(2) No increase in impact rate could be detected during the flyby at the asteroid Ida confirming earlier results from the Gaspra flyby.
(3) Within about 1.7 AU from Jupiter, intense streams of small dust particles were detected with impact rates of up to 20,000 per day whose impact directions are compatible with a Jovian origin. There is strong evidence that the dust stream particles are orders of magnitude smaller in mass and faster than the instrument's calibration, whereas the calibration can be safely applied to the bigger interstellar and interplanetary particles.
(4) Two different populations of dust particles were detected in the Jovian magnetosphere: (a) small stream particles during Galileo's approach to the planet with impact rates of up to 200 per day 3 days before Io flyby and (b) bigger particles concentrated closer to Jupiter between the Galilean satellites.
(5) The data from the dust instrument obtained within about 20 R_J from Jupiter (Jupiter radius, $R_J = 71{,}492$ km) show evidence for contamination by noise. The behavior of the impact directions of class 1 and class 2 events differs from that of class 3 events. Class 1 and 2 events from the Jovian system should therefore be treated with caution. Class 3 events do not show an indication for noise contamination and are considered good dust impacts.
(6) Noise tests performed regularly during the 3-year period did not reveal any change in the instrument noise characteristics. No degrading of the channeltron was revealed.

Acknowledgements

We thank the Galileo project at JPL for effective and successful mission operations. This work has been supported by the Deutsche Agentur für Raumfahrtangelegenheiten (DARA).

References

Baguhl, M., Grün, E. Linkert, D., Linkert, G., Siddique, N., 1993. Identification of 'small' dust impacts in the Ulysses dust detector data. Planet. Space Sci. 41, 1085–1098.

Baguhl, M., Grün, E., Hamilton, D.P., Linkert, G., Riemann, R., Staubach, P., Zook, H., 1995. The flux of interstellar dust observed by Ulysses and Galileo. Space Sci. Rev. 72, 471–476.

Baguhl, M., Grün, E., Landgraf, M., 1996. In situ measurements of interstellar dust with the Ulysses and Galileo spaceprobes. Space Sci. Rev. 78, 165–172.

D'Amario, L.A., Bright, L.E., Wolf, A.A., 1992. Galileo trajectory design. Space Sci. Rev. 60, 23–78.

Divine, N., 1993. Five populations of interplanetary meteoroids. J. Geophys. Res. 98, 17,029–17,048.

Grün, E., Fechtig, H., Hanner, M.S., Kissel, J., Lindblad, B.-A., Linkert, D., Linkert, G., Morfill, G.E., Zook, H.A., 1992a. The Galileo Dust Detector. Space Sci. Rev. 60, 317–340.

Grün, E., Fechtig, H., Giese, R.H., Kissel, J., Linkert, D., Maas, D., McDonnell, J.A.M., Morfill, G.E., Schwehm, G., Zook, H.A., 1992b. The Ulysses dust experiment. Astron. Astrophys. Suppl. Ser. 92, 411–423.

Grün, E., Baguhl, M., Fechtig, H., Hanner, M.S., Kissel, J., Lindblad, B.-A., Linkert, D., Linkert, G., Mann, I., McDonnell, J.A.M., Morfill, G.E., Polanskey, C., Riemann, R., Schwehm, G., Siddique, N., Zook, H.A., 1992c. Galileo and Ulysses dust measurements: From Venus to Jupiter. Geophys. Res. Letters 19, 1311–1314.

Grün, E., Zook, H.A., Baguhl, M., Balogh, A., Bame, S.J., Fechtig, H., Forsyth, R., Hanner, M.S., Horanyi, M., Kissel, J., Lindblad, B.-A., Linkert, D., Linkert, G., Mann, I., McDonnell, J.A.M., Morfill, G.E., Phillips, J.L., Polanskey, C., Schwehm, G., Siddique, N., Staubach, P., Svestka, J., Taylor, A., 1993. Discovery of jovian dust streams and interstellar grains by the Ulysses spacecraft. Nature 362, 428–430.

Grün, E., Hamilton, D.P., Baguhl, M., Riemann, R., Horanyi, M., Polanskey, C., 1994. Dust streams from comet Shoemaker-Levy 9? Geophys. Res. Let. 21, 1035–1038.

Grün, E., Baguhl, M., Fechtig, H., Hamilton, D.P., Kissel, J., Linkert, D., Linkert, G., Riemann, R., 1995a (Paper I). Reduction of Galileo and Ulysses dust data. Planet. Space Sci. 43, 941–951.

Grün, E., Baguhl, M., Divine, N., Fechtig, H., Hamilton, D.P., Hanner, M.S., Kissel, J., Lindblad, B.-A., Linkert, D., Linkert, G., Mann, I., McDonnell, J.A.M., Morfill, G.E., Polanskey, C., Riemann, R., Schwehm, G., Siddique, N., Staubach, P., Zook, H.A., 1995b (Paper II). Three years of Galileo dust data. Planet. Space Sci. 43, 953-969.

Grün, E., Baguhl, M., Divine, N., Fechtig, H., Hamilton, D.P., Hanner, M.S., Kissel, J., Lindblad, B.-A., Linkert, D., Linkert, G., Mann, I., McDonnell, J.A.M., Morfill, G.E., Polanskey, C., Riemann, R., Schwehm, G., Siddique, N., Staubach, P., Zook, H.A., 1995c (Paper III). Two years of Ulysses dust data. Planet. Space Sci. 43, 971–999.

Grün, E., Baguhl, M., Hamilton, D.P., Riemann, R., Zook, H.A., Dermott, S., Fechtig, H., Gustafson, B.A., Hanner, M.S., Horanyi, M., Khurana, K.K., Kissel, J., Kivelson, M., Lindblad, B.-A., Linkert, D., Linkert, G., Mann, I., McDonnell, J.A.M., Morfill, G.E., Polanskey, C., Schwehm, G., Srama, R., 1996a. Constraints from Galileo observations on the origin of Jovian dust streams. Nature 381, 395–398.

Grün, E., Hamilton, D.P., Riemann, R., Dermott, S., Fechtig, H., Gustafson, B.A., Hanner, M.S., Heck, A., Horányi, M., Kissel, J., Krüger, H., Lindblad, B.-A., Linkert, D., Linkert, G., Mann, I., McDonnell, J.A.M., Morfill, G.E., Polanskey, C., Schwehm, G., Srama, R., Zook, H.A., 1996b. Dust measurements during Galileo's approach to Jupiter and Io encounter. Science 274, 399–401.

Grün, E., Krüger, H., Dermott, S., Fechtig, H., Graps, A., Gustafson, B.A., Hamilton, D.P., Hanner, M.S., Heck, A., Horányi, M., Kissel, J., Lindblad, B.A., Linkert, D., Linkert, G., Mann, I., McDonnell, J.A.M., Morfill, G.E., Polanskey, C., Schwehm, G., Srama, R., Zook, H.A., 1997. Dust measurements in the Jovian magnetosphere. Geophys. Res. Lett. 24, 2171–2174.

Grün, E., Krüger, H., Graps, A., Hamilton, D.P., Heck, A., Linkert, G., Zook, H.A., Dermott, S., Fechtig, H., Gustafson, B.A., Hanner, M.S., Horányi, M., Kissel, J., Lindblad, B.-A., Linkert, D., Mann, I., McDonnell, J.A.M., Morfill, G.E., Polanskey, C., Schwehm, G., Srama, R., 1998. Galileo observes electromagnetically coupled dust in the jovian magnetosphere. J. Geophys. Res. in press.

Grün, E., Staubach, P., Baguhl, M., Hamilton, D.P., Zook, H.A., Dermott, S., Gustafson, B.A., Fechtig, H., Kissel, J., Linkert, D., Linkert, G., Srama, R., Hanner, M.S., Polanskey, C., Horanyi, M., Lindblad, B.-A., Mann, I., McDonnell, J.A.M., Morfill, G.E., Schwehm, G., 1997c. South-north and radial traverses through the zodiacal cloud. Icarus 129, 270–288.

Hamilton, D.P., Burns, J.A., 1992. Orbital stability zones about asteroids II. The destabilizing effects of eccentric orbits and of solar radiation. Icarus 96, 43-64.

Horányi, M., Grün, E., Heck, A., 1997. Modeling of the Galileo dust measurements at Jupiter. Geophys. Res. Lett. 24, 2175–2178.

Johnson, T.V., Yeates, C.M., Young, R., 1992. Space Science Reviews Volume on Galileo Mission Overview. Space Sci. Rev. 60, 3–21.

Krüger, H., Grün, E., Landgraf, M., Baguhl, M., Dermott, S., Fechtig, H., Gustafson, B.A., Hamilton, D.P., Hanner, M.S., Horányi, M., Kissel, J., Lindblad, B.-A., Linkert, D., Linkert, G., Mann,. I., McDonnell, J.A.M., Morfill, G.E., Polanskey, C., Schwehm, G., Srama, R., Zook, H.A., 1998. Three years of Ulysses dust data: 1993–1995. Planet. Space. Sci (Paper V).

Landgraf, M., Grün, E., 1998. In situ measurements of interstellar dust. In: Breitschwerdt, D., Freyberg, M.J., Trümper, J., (Eds). Proceedings of the IAU Collaquium No. 166 on The Local Bubble Beyond, Lecture Notes in Physics Vol. 506, Springer Heidelberg, pp. 381–384.

Riemann, R., Grün, E., 1992. Meteor streams, asteroids and comets near the orbits of Galileo and Ulysses. In: McDonnell, J.A.M., (Ed.), Proceedings of the workshop on Hypervelocity Impacts in Space, University of Kent at Canterbury, U.K., pp. 120–125.

Svestka, J., Auer, S., Baguhl, M., Grün, E., 1996. Measurements of dust electric charges by the Ulysses and Galileo dust detectors. In: Gustafson, B.A., Hanner, M.S., (Eds.). Physics, Chemistry and Dynamics of Interplanetary Dust, ASP Conference Series Vols. 104, pp. 31–34.

Zook, H.A., Grün, E., Baguhl, M., Hamilton, D.P., Linkert, G., Liou, J.-C., Forsyth, R., Phillips, J.L., 1996. Solar wind magnetic field bending of Jovian dust trajectories. Science 274, 1501–1503.